Methyltransferase DnmA is responsible for genome-wide N6-methyladenosine modifications at non-palindromic recognition sites in *Bacillus subtilis*

Taylor M. Nye, Lieke A. van Gijtenbeek, Amanda G. Stevens, Jeremy W. Schroeder, Justin R. Randall, Lindsay A. Matthews, and Lyle A. Simmons*

Department of Molecular, Cellular, and Developmental Biology
University of Michigan, Ann Arbor, Michigan USA.

*To whom correspondence should be addressed: Department of Molecular, Cellular, and Developmental Biology, University of Michigan, Ann Arbor, Michigan 48109-1055, United States. Phone: (734) 647-2016, Fax: (734) 615-6337
E-mail: lasimm@umich.edu

Running Title: *Bacillus subtilis* m6A affects gene expression
Keywords: DNA methyltransferase, gene expression, *Bacillus subtilis,* SMRT sequencing, SigA

Abstract

The genomes of organisms from all three domains of life harbor endogenous base modifications in the form of DNA methylation. In bacterial genomes, methylation occurs on adenosine and cytidine residues to include N6-methyladenine (m6A), 5-methylcytosine (m5C), and N4-methylcytosine (m4C). Bacterial DNA methylation has been well characterized in the context of restriction-modification (RM) systems, where methylation regulates DNA incision by the cognate restriction endonuclease. Relative to RM systems less is known about how m6A contributes to the epigenetic regulation of cellular functions in Gram-positive bacteria. Here, we characterize site-specific m6A modifications in the non-palindromic sequence GACG^{m}AG within the genomes of *Bacillus subtilis* strains. We demonstrate that the *yeeA* gene is a methyltransferase responsible for the presence of m6A modifications. We show that methylation from YeeA does not function to limit DNA uptake during natural transformation. Instead, we identify a subset of promoters that contain the methylation consensus sequence and show that loss of methylation within promoter regions causes a decrease in reporter expression. Further, we identify a transcriptional repressor that preferentially binds an unmethylated promoter used in the reporter assays. With these results we suggest that m6A modifications in *B. subtilis* function to promote gene expression.

Introduction

DNA methylation is pervasive across all three domains of life. In eukaryotes, 5-methylcytosine (m5C) modifications have been shown to function in development and the regulation of gene expression, with aberrant methylation implicated in human health, including cancer, autoimmune diseases, and metabolic disorders [for review, (1,2)]. m5C in promoter regions has been linked to the repression of downstream gene transcription, whereas gene body methylation has been positively correlated with gene expression [for review (3)]. A lesser-studied modification in the genomes of eukaryotes is N6-methyladenine (m6A). Recent studies have identified m6A in the genomes of *Chlamydomonas*, *Caenorhabditis elegans* and *Drosophila melanogaster* (4-6). In contrast to promoter m5C, m6A modifications appear to function in gene activation in the algae *Chlamydomonas* (4) and promoter m6A is also important in early *Drosophila* development (5). Further, m6A was positively correlated with gene expression in a diverse set of fungi (7). Thus, there is a growing recognition that m6A is critical for the regulation of gene expression in a broad range of eukaryotic organisms.

Bacterial genomes are known to harbor N4-methylcytosine (m4C) in addition to m5C and m6A [(8) and references therein]. All three modifications impart consequences to bacterial cells when methylation is lost (9). The most well understood example of DNA methylation in eubacteria is in the context of restriction-modification (RM) systems [for review (10,11)]. RM systems function as a bacterial host defense mechanism to prevent the invasion of foreign DNA, including phages and other mobile genetic elements (10,11). In organisms with RM systems, unmethylated foreign DNA is targeted for site-specific cleavage by a restriction endonuclease while the host chromosome is protected at the recognition sequence by site-specific DNA methylation (12). Methylation is achieved through the activity of DNA methyltransferases (MTases). MTases catalyze the transfer of a methyl group from the donor S-adenosylmethionine (SAM) to adenosine or

cytidine residues in DNA (13,14). MTases that lack a cognate endonuclease and do not function in RM systems are referred to as 'orphan MTases' (15). In a limited set of Gram-negative bacteria, orphan MTases have been shown to function in critical processes including cell cycle control (16), origin sequestration (17,18), DNA mismatch repair (19-21), and the regulation of gene expression [for review (22)]. DNA methylation from orphan and RM-based MTases has also been shown to establish epigenetic inheritance through phase variation primarily in Gram-negative pathogens (23-25). While much work has been done to characterize RM and orphan MTases from Gram-negative bacteria, much less is known about how m6A contributes to the regulation of the cell cycle or gene expression in Gram-positive bacteria (26).

Until recently, tools for unbiased detection and functional characterization of DNA methylation were limited. Available tools for detection, such as methylation-sensitive restriction endonuclease treatment and bisulfite sequencing, are limited to the sequence context and modification type that can be detected (27). The recent development of the Pacific Biosciences (PacBio) Single Molecule, Real-Time (SMRT) sequencing platform allows for detection of modifications without *a priori* knowledge of their existence (28). SMRT sequencing enables the analysis of real-time DNA polymerase kinetics for inference of DNA base modifications. Base modifications in the template strand result in changes in DNA polymerase kinetics compared to their unmodified counterparts, allowing for reliable, sequence-context specific detection of methylated bases during sequencing reactions (29). While differences in kinetic signatures for 5mC modified cytidine residues are modest, SMRT sequencing is adept for m6A and m4C detection (29).

Using the SMRT sequencing platform, a recent study of 230 diverse prokaryotes detected base modifications in 93% of the genomes surveyed (8). Of the genomes with detected modifications, 75% of the modifications were m6A, which is due in part to the

robust signal of m6A modifications in SMRT sequencing relative to other modifications (29). Given the high percentage of prokaryotic genomes with m6A detected and the contribution of m6A to the regulation of eukaryotic gene expression, it seems unlikely that the prevalent m6A modifications in prokaryotes are used exclusively in the context of regulating DNA cleavage by RM systems. As mentioned above, in *Escherichia coli* and *Caulobacter crescentus* m6A from orphan MTases occurs in palindromic recognition sequences and has been shown to mediate protein-DNA interactions (9,30), regulating important cellular processes including gene expression (31-34). Deletion of Dam methyltransferase (*dam*), which is responsible for m6A at GATC sites in *E. coli*, has severe pleiotropic effects (35,36). In *C. crescentus* deletion of the CcrM methyltransferase, which catalyzes the formation of m6A at GA(N)TC sites, is lethal when the CcrM-deficient strain is grown in rich media (16,37).

Much less is known about how m6A regulates cellular functions in Gram-positive bacteria. Recent work in *Streptococcus pyogenes* found that m6A from an active Type I RM system regulates virulence gene expression in a clinical isolate, suggesting that m6A could have important roles for regulating gene expression in Gram-positive systems (26).Therefore, the importance of m6A in *E. coli* and *C. crescentus* and the pervasive occurrence of m6A in prokaryotes (8) highlights the importance of understanding how m6A regulates cellular functions in the numerous and diverse set of bacterial genomes that contain the modification.

Here, we characterize m6A modifications in the Gram-positive bacterium *Bacillus subtilis* strains PY79 and NCIB 3610. Using SMRT sequencing, we show that m6A is present at non-palindromic GACG^{m}AG sites throughout the *B. subtilis* chromosome. Further, we characterize the methyltransferase, referred to herein as DnmA, as responsible for detectable m6A modifications in the *B. subtilis* genome of both strains. We found that DnmA does not function as part of an active, canonical Type I or Type II

RM system. Moreover, we show that the promoter regions for a subset of genes contain the consensus sequence and that loss of methylation in these *cis* regulatory elements results in a decrease in gene expression. Further, we show that the transcriptional repressor ScoC preferentially binds a promoter region that is unmethylated. Together, our results show that m6A can function as an epigenetic signal in *B. subtilis*.

Materials & Methods

General Bacteriology: The antibiotic concentrations used in this study are as follows: 5 µg/mL chloramphenicol, 0.5 µg/mL erythromycin, 100 µg/mL spectinomycin. Unless otherwise indicated, strains were grown in either LB (10 g/L tryptone, 5 g/L yeast extract, 10 g/L NaCl) or defined $S7_{50}$ minimal media supplemented with 1% glucose (1x $S7_{50}$ salts diluted from 10x $S7_{50}$ salts (104.7 g/L MOPS, 13.2 g/L ammonium sulfate, 6.8 g/L monobasic potassium phosphate, adjusted to pH 7 with potassium hydroxide), 0.1% potassium glutamate, 1% glucose, 40 µg/mL phenylalanine, 40 µg/mL tryptophan, 2 mM $MgCl_2$, 0.7 mM $CaCl_2$, 50 µM $MnCl_2$, 1 µM $ZnCl_2$, 1 µg/mL thiamine-HCl, 20 µM HCl, and 5 µM $FeCl_3$) at 30°C with shaking at 200 rpm.

Strain construction: The strains, plasmids and oligos used in this study can be found in Supplementary Tables S1, S2, and S3. Individual strain and plasmid construction can also be found in the Supplemental Materials and Methods. Deletions were created by ordering *Bacillus subtilis* 168 strains from the Bacillus Genetic Stock Center (http://www.bgsc.org/) where the respective genes were replaced with a *loxP* flanked erythromycin (erm) resistance cassette (BKE strains). Genomic DNA from the BKE strains was purified and used to transform *B. subtilis* strain PY79, and the erm resistance cassette was subsequently removed with Cre recombinase (38). Overexpression strains and all promoter GFP fusions were integrated in the PY79 *amyE*

locus via double crossover (39). Three colonies containing the crossover were selected and colony purified on LB plates containing 100 μg/mL spectinomycin. Successful integration of the constructs was verified by PCR, Sanger sequencing, and screening for the ability to utilize starch.

Chromosomal DNA purification: Genomic DNA for Pacific Biosciences SMRT sequencing was purified as follows. Strains were struck out on LB and grown overnight at 30°C. 500 mL LB cultures were inoculated at OD_{600} 0.05 and grown at 37°C. During mid-exponential phase (OD_{600} 0.6-0.8) an equal volume of methanol was added to each culture and centrifuged at 4,000 rpm for 30 minutes. The supernatant was discarded and cells were resuspended in 12.5 mL of 10% sucrose Tris/HCl pH 8 buffer and transferred to Oakridge tubes. Resuspensions were then treated with 310 μL lysozyme (40 mg/mL in 10% sucrose Tris/HCl pH 8 buffer) for 30 minutes at 37°C and mixed every 5 minutes. 1.25 mL of 0.5 M EDTA was added to each tube and incubated on ice for five minutes followed by addition of 10 mL of freshly prepared lysis solution (0.1% Triton X-100, 62.5 mM EDTA, 50 mM Tris/HCl pH 8). Solutions were centrifuged at 15,000 rpm for 30 minutes and decanted into chilled graduated cylinders. To each lysate 0.95 g/mL of cesium chloride (CsCl) was added and dissolved followed by a 1/10 volume addition of 10 mg/mL ethidium bromide. Solutions were balanced and centrifuged at 44,000 (131,600 x g) rpm for 24 hours. Chromosomal DNA was extracted and subjected to a second round of CsCl purification as described above. Solutions were centrifuged at 44,000 rpm (131,600 x g) for 48 hours. Ethidium bromide was removed by extraction 4x with water-saturated butanol. The aqueous phase was transferred to an Oakridge tube and 1 volume of water and 2 volumes ethanol were then added. The solution was centrifuged at 15,000 rpm for 20 minutes and the supernatant was aspirated. The pellet was washed with 70% ethanol and resuspended in 1 mL TE buffer.

In all other experiments, frozen strains were struck out and grown at 30°C. The plates were washed in $S7_{50}$ minimal media and 25 mL cultures were inoculated at an OD_{600} 0.05 and grown at 37°C with shaking to mid-exponential growth phase (OD_{600} 0.6-0.8). Genomic DNA was purified via phenol chloroform extraction method.

PacBio SMRT sequencing and methylation analysis: Chromosomal DNA was prepared for sequencing as described above. Library preparation and subsequent sequencing was performed as previously described (40,41). Modification and motif analyses were performed using RS_Modification_and_Motif_Analysis.1 version 2.3.0 with the appropriate *B. subtilis* reference genomes. The initial parameters used for modification analysis were performed using 0.75 minimum high quality reads, 50 bps minimum length, and a minimum ModQV call of 30. We also increased minimum high quality reads to >0.85 and minimum length to >1000 bps in subsequent analysis. Modification graphs were generated using functions from BaseModFunctions.v2.1.R available at: https://github.com/PacificBiosciences/Bioinformatics-Training/tree/master/basemods.

Motif Distribution Analysis: Motif distribution analysis was performed using the DistAMo web based server (42) available at http://computational.bio.uni-giessen.de/distamo searching the GACGAG motif for the *Bacillus subtilis* PY79 genome via accession number NC_022898.1.

Protein Purification (DnmA, DnmA (Y645A), and YabB): Recombinant proteins were purified from *E. coli* $BL21_{DE3}$ cells containing a pE-SUMO vector with the *B. subtilis* gene inserted (*dnmA, dnmA (Y465A)*, or *yabB*). Cultures were grown in 4 L of terrific broth (2.4% yeast extract, 1.2% tryptone, 0.4% glycerol, 250 mM $(NH_4)_2SO_4$, 500 mM KH_2PO_4,

1x metals (1,000x metals: 2.5 mM $FeCl_3$, 1 mM $CaCl_2$, 0.5 mM $ZnCl_2$, 0.1 mM $CoCl_2$, 0.1 mM $CuCl_2$, 0.1 mM $NiCl_2$, 0.1 mM Na_2MoO_4, 0.1 mM Na_2SeO_3, 1 mM H_3BO_3), and 25 µg/mL kanamycin) at 37°C with orbital rotation for 2 hours until reaching an OD_{600} of ~0.7. Overexpression was induced by adding IPTG to 1 mM and the cultures were grown for 3 additional hours 37°C. Cells were then pelleted by centrifugation and frozen in liquid nitrogen to be stored at -80°C. Once thawed, the pellet was resuspended in lysis buffer (50 mM Tris-HCl pH 8, 300 mM NaCl, 10% sucrose, 10 mM imidazole, 1x protease inhibitors (Roche 11873580001)) and cells were sonicated on ice. Cell debris was pelleted by centrifugation. Supernatant was then poured through a 3 mL Ni^{2+}-NTA agarose gravity-flow column. The column was washed with wash buffer (20 mM Tris-HCl pH 8, 10% glycerol, 20 mM imidazole, 2 M NaCl) and eluted with elution buffer (50 mM Tris-HCl pH 8, 150 mM NaCl, 400 mM imidazole). SDS-PAGE was performed to confirm the presence of desired protein. The sample was then dialyzed into anion exchange start buffer (50 mM Tris-HCl pH 8, 25 mM NaCl, 5% glycerol, 1 mM β-mercaptoethanol) and the sample was applied to a Q column (GE: 17115301) using an elution gradient of 50-750 mM NaCl. SDS-PAGE was performed and fractions containing desired protein were pooled and incubated with ULP1 protease at 25°C for 30 minutes. The digestion product was applied to another 3 mL Ni^{2+}-NTA gravity-flow column, washed, and eluted using the same buffers as above. SDS-PAGE was again performed to confirm the SUMO tag was removed and the protein was concentrated and buffer exchanged into protein storage buffer (50 mM Tris-HCl pH 8, 150 mM NaCl, 50% glycerol), aliquoted, flash frozen in liquid nitrogen, and stored at -80°C.

ScoC purification: Primers oTMN62 and 63 were used to amplify *scoC* from the *B. subtilis* chromosome and were subsequently combined with the pE-SUMO expression vector via Gibson assembly. Recombinant proteins were purified from *E. coli* $BL21_{DE3}$

cells grown in 2 L of LB with 25 µg/ml kanamycin at 37°C with orbital rotation until an OD_{600} of 0.7 was reached. Overexpression was induced by adding 0.5 mM IPTG followed by culture growth for an additional three hours at 37°C with orbital rotation and cultures were subsequently pelleted via centrifugation and stored at -80°C. The pellet was re-suspended in lysis buffer and sonicated on ice as described for DnmA and YabB. Subsequent to centrifugation, the supernatant was applied to a 4 mL Ni^{2+}-NTA agarose gravity-flow column. The column was washed with wash buffer (50 mM Tris-HCl pH 8, 25 mM imidazole, 2 M NaCl, 5% glycerol) and eluted with elution buffer (50 mM Tris-HCl pH 8, 400 mM imidazole, 150 mM NaCl, 5% glycerol). Following elution, 1 mM DTT and SUMO ULP1 protease were added to the elution fraction and incubated for 2 hours at room temperature. The sample was then dialyzed into storage buffer (50 mM Tris-HCl pH 8, 150 mM NaCl, 5% glycerol) overnight at 4°C. The dialyzed sample was then applied to another 4 mL Ni^{2+}-NTA gravity-flow column to separate the recombinant protein from the SUMO tag. SDS-PAGE was performed to confirm the SUMO tag was removed. Glycerol was added to 25% and the protein was aliquoted and flash frozen for storage at -80°C

Methylation Assays: All methylation reactions were performed in a buffer containing 50 mM Tris-HCl pH 8, 50 mM NaCl, and 200 µM $MgSO_4$. The following substrates were annealed in the same buffer at 2.5 µM concentration by heating primers to 100 °C for 30 seconds and then cooling to room temperature on the bench top: dsDNA target (oTNM38, oTMN39); dsDNA non-target (oTMN40, oTMN41); and dsRNA (oJR270, oJR271). The H^3-SAM (Perkin Elmer: NET155H001MC) was used at a concentration of 1 µM in solution. The purified DnmA, YabB, or DnmA (Y465A) was added to a concentration of 1 µM and all substrates were used at 0.25 µM in solution. The proteins were added in excess to determine if there was any off target methylation activity at

higher protein concentrations. The total reaction solution came to 10 µL. All reactions were incubated at 37°C for 150 minutes unless otherwise specified. Reactions were stopped using 450 µL of 10% TCA and placed on ice. The samples were filtrated using Glass microfiber filters (GE: 1822-025), washed with cold 70% ethanol, dried, and placed in a scintillation counter to measure mmol incorporation.

Growth Curves: Strains were plated on LB and grown overnight at 30°C. Plates were washed in LB and diluted to an OD_{600} of 0.05 in 10 mL of LB in side-armed flasks. Cultures were grown in shaking water baths at 37°C and optical density was measured using a Klett meter every half hour through late stationary phase. Growth curve experiments were done in triplicate and data was subsequently fit to a Gompertz growth (43) model $\{y = Aexp\{-exp\left[\frac{\mu_m \times e}{A}\ (\lambda - t) + 1\right]\}$ (where the parameters A, μ_m, and λ represent the time (t) when the growth rate equals zero (asymptote), the maximum growth rate, and the lag time, respectively), to obtain growth rate estimates (μ_m) for each strain.

Transformation efficiency assays: Strains were plated on LB and grown overnight at 30°C. Plates were washed with phosphate buffered saline (PBS) pH 7.4 and the cells were pelleted, the supernatant was aspirated, and a second PBS wash was completed before the cells were resuspended in PBS. The cells were used to inoculate a culture at an OD_{600} of 0.05 into 1 mL of 1x MC media (10x MC media: 615 mM K_2HPO_4, 380 mM KH_2PO_4, 1.11 M dextrose anhydrous, 30 mM sodium citrate dihydrate, 840 µM ferric ammonium citrate, 0.5 g casein hydrolysate, and 125 mM sodium aspartate monohydrate, to 50 mL with ddH_2O and filter sterilize) with 3 µL of 1M $MgSO_4$ and grown at 37°C with aeration for 4 hours. After 4 hours 3 µL of 1M $MgSO_4$ and 300 ng of pHP13

purified from *E. coli* MC1061 cells was added to 300 μL of cells and grown for an additional 1.5 hours at 37°C. 10x serial dilutions were performed into PBS and appropriate dilutions were plated onto LB plates for colony forming unit (CFU) counts and chloramphenicol plates for transformation forming unit (TFU) counts. Transformation efficiencies were calculated as TFU/CFU and the average transformation efficiency for replicates performed over three separate days was plotted along with the corresponding standard errors.

Flow Cytometry: Cells were grown overnight at 30°C on LB plates containing 100 μg/mL spectinomycin. Exponentially growing colonies were washed from the plates using $S7_{50}$ medium, and washed two more times to remove residual LB agar before diluting the cells in pre-warmed $S7_{50}$ medium to an OD_{600} of 0.05. Cells were grown to an OD_{600} of 0.4 at 30°C after which fluorescence of 200,000 cells was measured using an Attune™ NxT Acoustic Focusing Cytometer (ThermoFisher Scientific) using the following settings: Flow rate, 25 μL/min; FSC voltage, 200; SSC voltage, 250; BL1 voltage, 250.

Streptavidin pull-down: 5' biotinylated primers were used to amplify the 233 bp region of the *scpA* promoter via PCR using genomic DNA from strains LVG087 and LVG102 as a template, which correspond to the GACGAG and GACGTG promoter, respectively. To obtain total cell lysate, 4 L of strain TMN85 (Δ*dnmA*) was grown in $S7_{50}$ medium at 37°C with shaking until the culture reached an OD_{600} of 1.0. After the cells were harvested the pellets were washed with 1x PBS (pH 7.5) and then subsequently washed with Pull-Down Binding Buffer (PDBB; 50 mM Tris-HCl pH 7.5, 0.5 mM EDTA, 100 mM NaCl, 0.01% (v/v) Triton X-100, 25% (v/v) glycerol, and 1 mM DTT) and resuspended in ice-cold 20 mL PDBB supplemented with one tablet of cOmplete™, EDTA-free Protease

Inhibitor Cocktail (Roche, Mannheim, Germany). The cell suspensions were sonicated on ice (10s on, 40s off, 70 Hz) until the solutions cleared. Cell debris was removed from the lysate by two subsequent washing steps and the protein content of the supernatant was estimated using a Bradford assay (~20 mg/mL protein). For each pull-down experiment, 100 μL of Dynabeads™ M-270 Streptavidin magnetic bead slurry (ThermoFisher Scientific) was washed three times with 500 μL Pull-Down Wash Buffer (PDWB; 10 mM Tris-HCl pH 7.5, 1 mM EDTA, and 1 M NaCl). The beads were re-suspended in 250 μL PDWB, mixed with 200 pmol biotinylated probe DNA dissolved in 250 μL nuclease-free water, and incubated for 30 min at 25°C with gentle rotation. The DNA-coated beads were washed three times with PDBB before 100 mg protein and 100 μg salmon sperm DNA (Millipore Sigma) were mixed and added to the DNA-bound beads. After 2 hrs of incubation at room temperature with gentle rotation, the beads were separated and washed once with PDBB, once with PDBB plus 100 μg salmon sperm DNA, and again with PDBB. Bound proteins were eluted using Pull-Down Elution Buffer (PDEB; 50 mM Tris-HCl pH 7.5, 0.5 mM EDTA, 1 M NaCl, 0.01% (v/v) Triton X-100, 25% (v/v) glycerol, and 1 mM DTT). The eluted proteins were desalted and concentrated using TCA precipitation and separated on a 4-20% Mini-PROTEAN TGX precast protein gel (Bio-Rad, Hercules, USA). Bands in the 20 and 40 kDa size range were excised from the gel followed by protein identification using mass spectrometry through the University of Michigan Proteomics Resource Facility, project PRF-2019-L-SIMM-29.

ScoC EMSA: 5' IR dye end-labeled substrates oTN67/oTN68 and oTN70/oTN71, corresponding to the GACGAG and GACGTG oligos, respectively, were annealed at a concentration of 50 nM by heating at 95°C for 1 minute and then snap-cooled on ice. Care was taken to avoid subjecting the IR dye labeled oligos to light. Annealed oligos

were mixed at a final concentration of 5 nM with indicated concentrations of purified ScoC in 1x EMSA reaction buffer (5x EMSA reaction buffer: 250 mM Tris-HCl pH 8, 5 mM EDTA, 150 mM KCl, 10 mM $MgCl_2$, 5 mM DTT, 1% Tween 20, 125 µg/mL sheared salmon sperm DNA) to a final volume of 10 µL. Reactions were incubated at 37°C for 15 minutes and subsequently loaded onto and resolved via 6% Native-PAGE, which was performed covered and on ice for 60 minutes at 100V. The samples were visualized with the LI-COR Odyssey imager. The intensity of the shifted band was normalized to the no protein control for each sample to calculate the percent band shifted. Three replicates were completed and quantified across separate days and the average and standard errors for percent band shifted was reported in Figure 6.

Results

Characterization of *B. subtilis* PY79 and NCIB 3610 methylomes. It was previously published that *B. subtilis* does not have m6A at the *E. coli* Dam MTase recognition site, GATC, and that ectopic expression of Dam in *B. subtilis* induced the DNA damage response (44,45). However, until recently it remained unknown if *B. subtilis* contains m6A in another sequence context because the detection of m6A without *a priori* knowledge of the sequence context would require a new experimental approach. PacBio SMRT sequencing was used to determine if DNA modifications were present in the genome of several *B. subtilis* strains with the results deposited on the publicly available web resource REBASE maintained by New England Biolabs. This resource reports m6A occurring in various sequence motif contexts in 19 of 23 *B. subtilis* strains where SMRT sequencing was used. Among the *B. subtilis* strains analyzed, methylation at GACG^{m}AG sites was reported in four of the 23 strains (http://rebase.neb.com). Previously, our group performed PacBio sequencing on the widely used *B. subtilis* laboratory strain PY79 for whole-genome assembly (41). As part of our effort to study DNA methyltransferases, we

used PacBio sequencing to characterize the PY79 methylome. We purified genomic DNA from the wild type (WT) *B. subtilis* strain PY79 and analyzed our results using the SMRT sequencing platform, allowing for genome-wide base modification detection in sequence-specific contexts (29).

SMRT sequencing of the *B. subtilis* PY79 chromosome showed that the second adenosine residue within the sequence context 5'-GACG^{m}AG showed high modification quality values (modQVs), which indicates a statistically significant difference in DNA polymerase kinetics from the expected background at particular loci **(**Supplementary **Fig S1A, Table 1**). The interpulse duration (IPD) ratios, which are a comparison of DNA polymerase kinetics at a base within a particular sequence context compared to an unmethylated *in silico* control, were far higher for the second adenosine residue in the GACG^{m}AG motif compared to any other modified motifs in the *B. subtilis* chromosome (**Table 1,** Supplementary **Fig S1A**). Thus, we identify m6A in the sequence context 5'-GACG^{m}AG in the chromosome of *B. subtilis* PY79, herein referred to as the m6A motif.

We found that 99.7% of m6A motifs (1215/1219) were called as methylated in the PacBio SMRT sequencing analysis at the 3'-adenosine during exponential growth in defined minimal medium. While our sequencing analysis identified other motifs in the *B. subtilis* PY79 chromosome, the average modQVs, IPD ratios, and the percentage of motifs called as modified were far lower compared to m6A identified within the GACG^{m}AG sequence (Supplementary **Table S4** and **Fig S2**). It is likely that most of the other motifs called represent DNA secondary structures that affect DNA polymerase kinetics or sequencing noise instead of genuine nucleic acid modifications (Supplementary **Table S4**). For completeness we chose to report all motifs called during analysis of the SMRT sequencing data (Supplementary **Table S4**).

Of the 1,219 m6A motifs that occur in the *B. subtilis* PY79 genome, 1,118 (91.7%) occur in protein coding regions. Intergenic regions, which compose 11.2% of the genome, contain 7% (85 motifs in 76 regions) of the m6A motifs. With the exception of only a few sites, the majority of m6A sites had greater than 75% of sequencing reads called as methylated independent of genome position or occurrence on the plus or minus strand of the chromosome (Supplementary **Fig S2** and Supplementary **Table S4**).

B. subtilis PY79 is a commonly used laboratory strain, however selection in the lab has caused PY79 to lose many of the robust phenotypes associated with ancestral strains of *B. subtilis* (46). To determine whether m6A is present in the ancestral strain, we purified genomic DNA from *B. subtilis* strain NCIB 3610 (40) for SMRT sequencing and found m6A within the same GACGAG sequence context **(**Supplementary **Fig S1B** and **Table 1)**. In NCIB 3610 94.7% (1208/1275) of m6A sites were called as methylated in the PacBio SMRT sequencing analysis. The chromosome of the ancestral strain is considerably larger than PY79 and harbors an 84-kb plasmid, both of which account for the increased number of m6A motifs (40). The decrease in the percentage of motifs called as modified between PY79 and NCIB 3610 (99.7% → 94.7%) could be the result of biological variation, such as an increase in protein binding or other factors that may occlude methylation of recognition sites. The decrease in motifs called could also be due to technical variation in sequencing reactions. We note that we also detected many additional motifs in the ancestral strain that did not appear in the lab strain PY79, with each motif called listed in supplementary **Table S4**. Further, m6A at GACGAG sequences has also been reported for three *B. subtilis* strains other than PY79 and NCIB 3610 on REBASE.

In addition to m6A modifications, SMRT sequencing of the PY79 genome identified cytidine modifications in the sequence ^{m}CTCGARB (where R represents a purine and B either a cytidine or a guanosine). These results are described in the

supplementary results section, where we show using methylation-sensitive restriction digest that m5C formation occurs in the *B. subtilis* PY79 genome through the BsuMI RM system **(**Supplementary **Figure S3)** previously described for *B. subtilis* Marburg (47).

Distribution of m6A sites across the *B. subtilis* genome shows enrichment on the lagging strand of the left chromosomal arm. To begin to understand the function of m6A in *B. subtilis*, we used the motif enrichment program DistAMo (42) to determine the location of m6A sites on the *B. subtilis* chromosome. This was done to determine if m6A sites are uniform or showed areas of enrichment and de-enrichment throughout the chromosome **(Fig 1)**. We present the analysis using sliding windows of 50 kb to 500 kb over the length of the chromosome by the rings from outside (large) to inside (small) scaling in 50 kb increments. Over (red) and under (blue) enrichment are colored by z-scores in the scale as shown. From the analysis we determine that the locations of m6A sites are certainly not uniform across the chromosome and instead show patterns of enrichment in particular regions. We find that several areas are largely devoid of m6A sites, including the terminus region and the origin of replication **(Fig 1)**. Analysis of enrichment shows that locations in the *B. subtilis* chromosome with high z-scores includes the right and left chromosomal arms with the largest enrichment on the lagging strand of the left chromosomal arm **(Fig 1C)**. With these results we suggest that m6A is unlikely to function in origin sequestration or DNA mismatch repair as described for Dam methylation in *E. coli* (17,18) due to our finding that the origin does not contain m6A sites and because m6A is non-palindromic and not uniform across the *B. subtilis* chromosome. To be certain, we empirically test if m6A contributes to replication timing, mutagenesis, or recombination in the supplementary results and show no effect (Supplementary **Figure S4, Figure S8** and Supplementary **Table S5**).

Methyltransferase YeeA is necessary for m6A formation *in vivo*. DNA methylation is catalyzed by DNA methyltransferases (MTases) (48). To identify putative MTase(s) responsible for the observed m6A modification, we searched all protein coding sequences for the conserved DNA m6A MTase catalytic motif (D/N/S)PPY (48). This search yielded two uncharacterized MTases, coded for by the genes *yabB* and *yeeA* (*dnmA*) (41). We created clean deletions of the Δ*yabB* and Δ*yeeA* (*dnmA*) coding regions as well as a Δ*yabB*Δ*yeeA* double deletion. Each of these strains was viable and none of the deletions conferred a growth defect on *B. subtilis* under the conditions used here **(Fig 3A,** described later in the results**)**.

To identify the MTase responsible for genomic m6A, DNA was harvested from each strain when cultures reached an OD_{600} of ~0.7 followed by SMRT sequencing. Subsequent methylation analysis revealed that chromosomal DNA from Δ*yeeA* (*dnmA*) cells lost all detectable methylation at the m6A motif previously identified in WT cells in both PY79 and NCIB 3610 strain backgrounds **(Table 2,** Supplementary **Fig S5,** and Supplementary **Tables S6, S7 and S8** for all PY79 Δ*yeeA* (*dnmA*) GACGAG sites**)**. Expression of *yeeA* (*dnmA*) from an ectopic locus in the Δ*yeeA* (*dnmA*) background restored methylation at the m6A site **(**Supplementary **Fig S5C** and **Table 2).** Computational analysis from sequencing data posted on REBASE also predicted YeeA (DnmA) as the MTase responsible for m6A detected in strains of *B. subtilis* with modifications at the m6A motif described here.

Genomic DNA from Δ*yabB* cells retained the methylation at m6A sites **(**Supplementary **Fig S6,** Supplementary **Table S9)** whereas detectable modifications at the m6A site were lost in the double deletion strain **(**Supplementary **Fig S6B,** Supplementary **Table S9)**. Interestingly, while methylation is maintained at the m6A site in the Δ*yabB* strain, we noticed additional motifs not present in the WT or Δ*yeeA* (*dnmA*) strains that were detected upon loss of *yabB* in the single or double deletion strains

(Supplementary **Table S9**). These additional motifs are likely to result from sequencing noise and/or DNA secondary structure given the low IPD ratios (Supplementary **Table S9**). With these results we show that *yeeA* (*dnmA*) is necessary for genomic m6A formation in the sequence context GACG^{m}AG *in vivo* and we refer to YeeA herein as DNA methyltransferase A (DnmA), with the formal name of M.BsuPY79I and M.Bsu3610I for strains PY79 and NCIB 3610, respectively. For simplicity, we will collectively refer to M.BsuPY79I and M.Bsu3610I as DnmA in the work presented below.

DnmA is sufficient for methylation of m6A sites in double stranded (ds)DNA *in vitro*. DNA MTases typically use SAM to catalyze the transfer of a methyl group to a DNA base (9). DnmA (M.BsuPY79I), YabB, and a DnmA catalytically inactive variant (Y465A) were purified **(Fig 2A)**. In addition to the predicted ~120-kDa band corresponding to the DnmA monomer, a high molecular weight species was observed in the DnmA purifications. The slower migrating protein was analyzed by mass spectrometry identifying it as multimer of DnmA. We speculate that the DnmA multimer is caused by irreversible disulfide bonding or another crosslink that forms between two purified DnmA monomers during isolation **(**Supplementary **Table S10)**.

A time course methylation experiment was performed to determine if DnmA is sufficient to catalyze methylation of the m6A motif in DNA **(Fig 2B)**. The purified proteins were incubated with tritiated SAM and an oligonucleotide sequence from the *B. subtilis addA* locus containing the m6A (target) motif. Incorporation of the labeled methyl group over time indicates that DnmA is indeed sufficient for methylation at m6A motifs in dsDNA **(Fig 2B)**. With the results from the time course methylation experiment we suggest that purified DnmA does not have significant activity on single-strand (ss)DNA. As a control we show that the Y465A catalytically inactive variant was unable to methylate the substrate indicating that the MTase activity we detect is specific to DnmA.

With the *in vitro* methylation assay established, we tested the activity of DnmA and YabB on DNA containing the target sequence and whole cell RNA extracted from a Δ*dnmA*Δ*yabB* double mutant strain by assaying for incorporation of methylation from tritiated SAM. As expected, DnmA showed activity on the dsDNA substrate with the target sequence, but had minimal activity when whole cell RNA was used as a substrate **(Fig 2C)**. In support of the *in vivo* results, we show that purified YabB had very little activity on a DNA substrate, whereas YabB did show incorporation when whole cell RNA was used as a substrate. With these results we suggest that YabB may function as an RNA methyltransferase **(Fig 2C)**. To test if the m6A motif was necessary for DnmA methylation *in vitro*, the 3'-adenosine residue was substituted with thymidine (non-target sequence) and incubated with DnmA and tritiated SAM. As shown in **Fig 2D**, there was no appreciable incorporation of the methyl group by DnmA to the non-target sequence, demonstrating that methylation is specific for the target sequence (m6A motif). We also tested DnmA for methylation of dsRNA, ssDNA, and ssRNA bearing the target sequence. The results show little to no methylation for any of these substrates with the exception of ssDNA, which yielded only weak methylation activity relative to dsDNA **(Fig 2D)**. Together, these results provide strong evidence that DnmA is specific for dsDNA containing the m6A motif.

To determine if the lack of methylation at the non-target sequence was caused by an inability of DnmA to bind DNA, an electrophoretic mobility shift assay (EMSA) was performed on 5' end-labeled target (GACGAG), non-target (GACGTG), and a degenerate sequence where the entire target sequence had been removed. Incubation of DnmA with the target, non-target, and degenerate sequences each resulted in a shift, indicating that the methylation specificity is not due to a loss of DNA binding at other sequences **(**Supplementary **Fig S7)**. Additionally, the Y465A catalytically inactive variant

still bound the target sequence, suggesting that this variant is only dysfunctional for methyltransferase activity **(**Supplementary **Fig S7)**. We conclude that DnmA is necessary and sufficient to methylate dsDNA that carries the GACGAG sequence *in vivo* and *in vitro* and that Y465 is an important residue for activity.

DnmA does not function as part of an active RM system. We next asked if DnmA functions as part of an active RM system. DnmA shares 38% identity and 57% similarity with the MmeI enzyme, which is a bifunctional protein with a methyltransferase domain and a PD-ExK endonuclease motif in the amino terminal domain. MmeI belongs to a subgroup of Type II RM systems that use DNA hemi-methylation for host chromosome protection (49). DnmA was included in a set of MmeI homologs that lack the endonuclease motif in the amino terminal domain but are flanked by conserved genes similar to *yeeB* and *yeeC*, which are immediately downstream of *dnmA* (49). It was found that under the conditions tested for other MmeI homologs DnmA lacked endonuclease activity, however it is important to note that the downstream *yeeB* and *yeeC* gene products are annotated as a putative helicase and an endonuclease, respectively (49). Deletion of *dnmA* does not result in a growth defect **(Fig 3A)**, which would suggest that *yeeB* lacks endonuclease activity associated with typical Type II RM systems, where endonuclease activity is achieved independent of the MTase.

It has been suggested that DnmA, along with YeeB and YeeC, comprise a Type I-like RM system, where restriction endonuclease activity requires the MTase subunit and DNA cleavage would not occur efficiently in the absence of DnmA (49). To test this possibility, we performed a transformation efficiency assay in WT and Δ*dnmA* cells with the plasmid pHP13, which is a 4.7 kb plasmid containing three m6A sites as the donor DNA **(Fig 3B)**. Plasmid purified from *E. coli* cells was used to transform competency deficient (Δ*comK*), hyper-competent (Δ*rok*), WT and Δ*dnmA* strains followed by

selection for transformants conferring resistance to chloramphenicol. We found that compared to Δ*comK* and Δ*rok* strains, with transformation efficiencies of < 1 $x10^{-8}$ and 177 $x10^{-5}$ (SE 13.2 $x10^{-5}$), respectively, the transformation efficiencies of WT [7.33 $x10^{-5}$ (SE 3.30 $x10^{-6}$)] and Δ*dnmA* [9.44 $x10^{-5}$ (SE 1.25 $x10^{-5}$)] were nearly indistinguishable (**Fig 3C**). We show that DnmA, YeeB, and YeeC do not function to restrict DNA update during natural genetic competence. Based on the transformation results and the conservation of these three genes clustering together, we suggest that DnmA, YeeB, and YeeC could be part of an inactive or inefficient Type I-like RM system or perhaps a noncanonical RM system. We also cannot exclude the possibility that restriction activity could be measured under some other circumstance, such as phage predation.

Proximity of m6A sites to -35 boxes of housekeeping sigma factor SigA regulates promoter activity. Due to the enrichment of m6A within particular genomic locations (**Fig 1**), we considered a role for m6A in regulating gene expression. Several prior studies have shown that DNA methylation from RM systems can also regulate gene expression (23,25,26). Accordingly, DNA MTase targets that occur within promoter or operator regions have the potential to influence transcription (50). Thus, we hypothesized that DnmA-dependent methylation might exhibit a similar function in *B. subtilis*.

To identify genes that might be affected by DnmA-dependent methylation, we used the list of transcribed regions 5' of *B. subtilis* 168 open reading frames (ORFs) reported previously (51) to prioritize the subset of promoters in *B. subtilis* with m6A sites located on the left chromosomal arm where we observed m6A enrichment. The promoters chosen for analysis included those of non-coding and anti-sense RNAs as well as promoters embedded inside transcriptional units and we excluded promoters where the target site occurs downstream of the transcriptional start site **(**Supplementary

Table S11). *B. subtilis* PY79 contains 32 transcribed regions 5' of ORFs with the m6A motif in the vicinity of known or predicted sigma factor binding sites **(**Supplementary **Table S11)**. To examine if m6A in promoter regions influences gene expression in *B. subtilis*, we constructed a series of transcriptional fusions where a *gfp* allele was introduced downstream of the respective m6A motif-containing promoter **(Fig 4A)**. All transcriptional fusions were introduced at the ectopic *amyE* locus to separate the promoter from other potential *cis*-acting regulatory elements or chromosome structure contexts that could affect expression **(Fig 4B)**. Promoter activity was monitored in WT and Δ*dnmA* strains using fluorescence as a reporter in single cells during mid-exponential growth by flow cytometry (please see Materials and Methods).

We found that loss of m6A in a subset of *B. subtilis* promoters, specifically those that contain an m6A motif in or slightly downstream of the -35 region of the SigA-binding box (*PscpA, Phbs, PrnhC, PyumC, PzapA*), consistently resulted in decreased activity from the unmethylated promoter relative to the methylated counterpart **(Fig 4C** and **D)**. The m6A sites in the promoter region for *PscpA, Phbs, PrnhC, PyumC, PzapA* in PY79 are identical to the promoter regions in *B. subtilis* strain NCIB 3610.

We did not observe this trend for the promoter fusions that contained m6A sites away from the -35 box. For example, the activation level of the SigB-inducible *rsbV-rsbW-sigB-rsbX* promoter (PrsbV), with an m6A site directly upstream of the -10 box, was not influenced by the presence of methylation during normal growth or even after stressing the cells with 4% ethanol for 1-hour as described (52) **(Fig 4C** and **D)**. Similarly, we did not observe differences in *gfp* expression with the *PcomEA*, *PwprA*, or *PyloA* fusions in the Δ*dnmA* background relative to WT.

The m6A motif was present just upstream and overlapping the -35 region of the SigA binding box for *PzapA* (transcription unit: *zapA-yshB-polX-mutSB-yshE*) and

PyumC, respectively, and both reporters showed a decrease in activity in Δ*dnmA* cells relative to WT (**Fig 4C** and **D**). ZapA is involved in FtsZ ring assembly and YumC is an essential ferrodoxin/flavodoxin reductase (53,54). The m6A site for the remaining three promoter fusions that showed decreased expression upon loss of m6A, *PscpA* (transcription unit: *scpA-scpB-ypuI*), *Phbs* (transcription unit: *S861-hbs*), and *PrnhC*, was located just downstream of the -35 region of the SigA binding box. Interestingly, the gene products for two of the differentially expressed promoter regions, *scpA* and *hbs*, have important roles in chromosome segregation, chromosome structure, and organization (55-60). The changes in *Phbs* activity were mild, which is likely due to the fact that *Phbs* contains two SigA-binding boxes, of which the m6A-positive box is the least dominant of the two promoters (61). Another promoter fusion that exhibited a DnmA-dependent increase in expression was P*rnhC*, which codes for RNase HIII, an enzyme important for cleavage of RNA-DNA hybrids (62,63). One type of RNA-DNA hybrid is an R-loop, which could affect local chromosome structure and transcription (64). Together, decreased expression from *PscpA*, *Phbs*, and *PrnhC* could have impacts on global chromosome structure, altering the expression of other genes.

To further investigate how m6A methylation affects transcription, the m6A site within the P*scpA*-GFP promoter was mutated to GACG**C**G, ensuring loss of methylation at this site in both the WT and Δ*dnmA* backgrounds. The GACG**C**G containing promoter adopted the same activity as observed in the Δ*dnmA* strain, indicating that m6A at the fifth position of the motif stimulates gene expression (**Fig 5A** and **B**). Interestingly, an A→T at the fifth position of the m6A site (GACG**T**G) made P*scpA*-GFP behave as if it were m6A (GACG^{m}AG) in both WT and Δ*dnmA* backgrounds **(Fig 5A** and **B** middle panel**).** The reason for how thymidine in the fifth position of the motif stimulates gene expression to the same extent as m6A is unclear. To further test how integrity of the motif modulates P*scpA* activity, the motif was subsequently changed to GACGA**C** so

that the fifth position was unchanged but the DnmA recognition site was lost. The promoter adopted the same activity as quantified in the Δ*dnmA* strain, indicating that m6A or T at the fifth position of the motif stimulates gene expression for the *scpA* promoter **(Fig 5A** and **B)**. With these data we suggest that m6A is capable of regulating gene expression when located near the -35 binding site for SigA with methylation promoting gene expression from a subset of promoters in *B. subtilis.*

Transcriptional repressor ScoC binds GACGAG sites. The mechanism for m6A-dependent promotion of gene expression could be explained by an increase in SigA binding at methylated promoter regions or a less direct mechanism, such as competition for SigA binding with a methylation-sensitive transcriptional regulator. To determine if proteins in *B. subtilis* differentially associate with unmethylated DNA, we performed a pull-down in cell extracts using two different oligos. We amplified biotinylated oligos corresponding to the *PscpA* promoter region containing the GACGAG site. We could not obtain complete methylation of the substrate *in vitro* using purified DnmA. Therefore, we amplified the region and introduced a mutation in the m6A motif to GACG**T**G, which behaved like the WT methylated promoter in our reporter assay using the same promoter region **(Fig 5A-B, middle panel)**. We isolated protein lysates from exponentially growing *B. subtilis* cells, incubated the lysates with our biotinylated oligos, performed a streptavidin pull-down, and visualized the proteins from each pull-down experiment via SDS-PAGE. We noted differences in the protein bands for the GACGAG relative to GACGTG oligo in the 20 and 40 kDa molecular weight range. These regions were excised from the gel and the proteins identified using mass spectrometry. Of the top four most abundant proteins across the samples, the transcriptional regulator of the transition state, ScoC (65,66), was the only protein that did not appear in both pull-down experiments **(Fig 6A)**. We found that ScoC was only present in the pull-down with the

oligo that contained the GACGAG site, representing the unmethylated promoter state. No peptides corresponding to ScoC were identified in the pull-down of the GACG**T**G control site **(Fig 6A)**.

To directly test if ScoC binding is affected by the A→T mutation, we purified ScoC **(Fig 6B)** and performed electrophoretic mobility shift assays (EMSAs). We used labeled oligos representing the *PscpA* promoter that only differed in the GACGAG and GACGTG sites, which overlap the -35 box but occur just outside of the ScoC consensus binding site **(Fig 6C)**. The intensity of the shifted band was quantified and normalized to a no protein control for three independent experiments across a range of protein concentrations and the percent band shifted was compared at 250 nM and 500 nM ScoC. Consistent with the results from our pull-down experiment, we observed a 33.4% (S.E. ±2.6) and 14.7% (S.E. ±1.1) percent band shift at 250 nM ScoC for the GACGAG and GACGTG oligos, respectively **(Fig 6D-E)**. We also observed percent band shifts of 70.6% (S.E. ±9.0) and 45.7% (S.E. ±5.1) at 500 nM ScoC for the GACGAG and GACGTG oligos, respectively **(Fig 6D-E)**. The increased binding of ScoC to the oligo with the GACGAG site compared to the oligo with the GACGTG site **(Fig 6E)** and the decrease in expression we observed from the GACGAG promoter region compared to the GACGTG or GACG^{m}AG promoter **(Fig 5)** supports the model that ScoC is a transcriptional repressor (65,66) and that ScoC shows preferential binding to an unmethylated promoter with the m6A site proximal to the ScoC binding site. With these results we suggest that ScoC binds to unmethylated GACGAG sites in promoter regions repressing transcription. When the GACGAG site overlaps or is adjacent to the ScoC binding site we suggest that methylation or A→T mutation at the fifth position could weaken ScoC binding leading to an increase in gene transcription.

Discussion

We report that DnmA (M.BsuPY79I or M.Bsu3610I) is responsible for endogenous m6A modifications that promote gene expression in *B. subtilis* strain PY79. We have shown that m6A in *B. subtilis* occurs at non-palindromic GACG^{m}AG sites in the chromosome with enrichment on the left chromosomal arm. In *B. subtilis* PY79 there are only 1,219 chromosomal m6A sites in contrast to the ~20,000 and ~4,500 palindromic m6A sites in *E. coli* and *C. crescentus,* respectively (67,68). While non-palindromic sites have been described (8) and have been shown to affect gene expression (25), the palindromic nature of m6A sites in *E. coli* and *C. crescentus* is necessary for function in DNA mismatch repair, origin sequestration, and cell cycle control (67). During these processes, protein binding or activity is dictated by full versus hemi-methylated states of m6A motifs, which determines the downstream regulatory role (67,69). Here, we have shown that loss of m6A at the non-palindromic GACG^{m}AG sites in *B. subtilis* also affects the regulation of gene expression, with loss of methylation resulting in decreased expression of genes, including *scpA* and *hbs*, which code for proteins important for chromosome structure, organization, and maintenance (55-60) (**Fig 4C** and **D**). Our data indicate that the presence of m6A promotes the expression of a subset of genes in PY79 that could have important downstream effects on gene expression and chromosome structure.

One mechanism by which m6A regulates gene expression is through dictating transcription factor binding to promoter regions. In prototypical *E. coli* the methylation state of recognition sites for Dam methyltransferase in promoter regions has been shown to affect expression of a subset of genes, including virulence factors (67,69). One such example is the *agn43* promoter, where methylation at the promoter blocks binding of the redox sensitive repressor OxyR, thereby stimulating production of Agn43, which is important for non-fimbrical adhesion (70). Also, uropathogenic *E. coli* use phase

variation to evade the host immune system by altering the expression of the pyelonephritis-associated pilus (pap) in a Dam methylation dependent manner (24). In the Gram-negative pathogen *Neisseria meningitidis* non-palindromic m6A sites from an active Type III RM system also function in phase variation (25). The Gram-negative bacterium *C. crescentus* has a transcriptional activator, GcrA, which associates with RNA polymerase-σ^{70} and recognizes a subset of promoter regions that are methylated at palindromic recognition sites by the CcrM MTase (71).

Here we have demonstrated that m6A regulated promoters in *B. subtilis* PY79 contain the methylation site at or slightly downstream of the -35 region of the housekeeping SigA binding site (72). We have shown that, in the absence of modification at the m6A site, we observe increased binding of the transcriptional repressor ScoC in the promoter region for the gene *scpA* **(Fig 6A-E)**. The increased binding of the transcriptional repressor ScoC at the *scpA* promoter containing a GACGAG site relative to the GACGTG site supports our reporter results, showing that the GACGTG site phenocopied the higher expression levels in a wild type strain relative to the Δ*dnmA* strain **(Fig 5A-B)**. We speculate that increased binding of the ScoC repressor to unmethylated GACGAG sites is responsible for the decreased gene expression we observe from the *scpA* promoter, representing one mechanism by which m6A could regulate gene expression in *B. subtilis* PY79.

While m6A-mediated binding of ScoC represents one mechanism by which m6A regulates gene expression, we find it likely that many other mechanisms exist. The methylation-responsive promoters identified in the current study do not share an obvious ScoC consensus binding sequence. Future work will be necessary to determine the additional regulatory mechanism(s) that result in increased gene expression at methylated promoter regions in *B. subtilis* PY79 and 3610.

Each of the promoter fusions tested was ectopically expressed at the *amyE* locus, which allowed us to assay for the effect of promoter methylation status independent of the effects of chromosomal location and local chromosome architecture. This experimental design allows for identification of promoter region activities that were affected by loss of methylation at the m6A site but did not account for other factors. Interestingly, as shown **(Fig 4B)**, the genes for many of the downregulated promoter fusions occur toward the terminus (*hbs*, *scpA*, *rnhC*, and *zapA*) and on the left arm of the chromosome, whereas the *amyE* locus is origin proximal and occurs on the right arm of the chromosome. Thus, we are able to conclude that methylation at the m6A site in *B. subtilis* PY79 promotes gene expression for a subset of genes but we cannot rule out other factors that control gene expression at the endogenous loci or indirect regulatory functions of m6A elsewhere in the chromosome.

In addition to its direct regulatory function at select promoter regions, m6A may have indirect effects on gene expression. It has been shown that m6A can increase the curvature of the DNA that may, in turn, influence protein binding and chromosome architecture (73,74). Alternatively, m6A might directly influence the expression of DNA binding proteins that contribute to chromosome architecture. Consistent with this hypothesis, we observe slight but significant downregulation of the *hbs* gene, which codes for the essential and highly abundant histone-like protein HBsu **(Fig 4C)**. A potential decrease in HBsu levels concomitant with the preference of HBsu for highly curved regions of DNA creates the possibility for an m6A-dependent mechanism for changes in overall DNA topology and chromosome architecture. Thus, loss of m6A may affect protein occupancy throughout the chromosome to influence chromosome architecture in such a way that results in more changes to gene expression. It is important to note that both direct and indirect models of m6A-dependent changes are possible and that they are not mutually exclusive

Genomic m6A from orphan and active RM system MTases has been shown to function in the regulation of gene expression [e.g. (23-26)]. Here we demonstrate that loss of MTase DnmA does not affect the natural transformation efficiency of foreign methylated DNA from a plasmid with multiple recognition sites in competent cells. Therefore, we suggest that DnmA is an MTase from an inefficient or inactive RM system. We have also discovered that DnmA-dependent m6A in the promoter regions of a subset of genes promotes gene expression in *B. subtilis* PY79 and we show that transcriptional repressor ScoC binds unmethylated DNA. In addition to influencing ScoC binding, we find it interesting that m6A promotes expression of several genes involved in chromosome structure and maintenance, which could in turn have effects on the expression of other genes. In total, we have shown that DNA methylation from DnmA has an effect on gene expression, prompting further investigation of RM systems and their possible regulatory contribution outside of DNA restriction.

Data Availability

The SMRT sequencing data for PY79 and 3610 are available (40,41) with accession number CP006881 for PY79 and accession numbers CP020102 for the NCIB 3610 chromosome and pBS32 plasmid CP020103. The SMRT sequencing data for PY79 strains Δ*dnmA*, Δ*yabB*, P_{spac}*dnmA*; Δ*dnmA,* Δ*dnmA*Δ*yabB*, and NCIB 3610 strain Δ*dnmA* is available [GEO GSE130695] at https://www.ncbi.nlm.nih.gov/geo. The raw data, equations, and descriptions of calculations used to generate Supplementary Figure S4F and Supplementary Table S5 have been deposited to http//figureshare.com DOI 10.6084/m9.figshare.8070995 and are publicly available.

Supplementary Data

Supplementary data includes Figures S1-S8 and Tables S1-S11.

Funding

This study was supported by National Science Foundation grant MCB 1714539 to LAS. TMN was supported by a National Science Foundation predoctoral fellowship (#DEG 1256260). JWS was supported in part by a predoctoral fellowship from the National Institutes of Health Genetics Training Program (T32 GM007544) and Associate Professor Funds from the LS A at the University of Michigan to LAS. JRR was supported in part by NIH Cellular Biotechnology Training Program (T32 GM008353) and a predoctoral fellowship from the Rackham Graduate School at the University of Michigan. AGS was supported by a summer fellowship from MCDB at the University of Michigan.

Conflict of interest statement. None declared.

Acknowledgements

The authors would like to thank the Simmons lab as well as Daniel Kearns and Reid Oshiro for helpful discussions and critical input during the progression of this work.

Author Contributions

Experiments were designed by TMN, LVG, JRR, JWS, and LAS. Experiments were performed by TMN, LVG, AGS, JRR, JWS, LAM, and LAS. Data were analyzed by TMN, LVG, AGS, JRR, JWS, LAM, and LAS. The first draft of the manuscript was written by TMN, LVG, and LAS. All authors contributed to editing and finalization of the manuscript.

References

1. Chen, K., Zhao, B.S. and He, C. (2016) Nucleic Acid Modifications in Regulation of Gene Expression. *Cell Chem Biol*, **23**, 74-85.

2. Jin, Z. and Liu, Y. (2018) DNA methylation in human diseases. *Genes Dis*, **5**, 1-8.

3. Jones, P.A. (2012) Functions of DNA methylation: islands, start sites, gene bodies and beyond. *Nat Rev Genet*, **13**, 484-492.

4. Fu, Y., Luo, G.Z., Chen, K., Deng, X., Yu, M., Han, D., Hao, Z., Liu, J., Lu, X., Dore, L.C. *et al.* (2015) N6-methyldeoxyadenosine marks active transcription start sites in Chlamydomonas. *Cell*, **161**, 879-892.

5. Zhang, G., Huang, H., Liu, D., Cheng, Y., Liu, X., Zhang, W., Yin, R., Zhang, D., Zhang, P., Liu, J. *et al.* (2015) N6-methyladenine DNA modification in Drosophila. *Cell*, **161**, 893-906.

6. Greer, E.L., Blanco, M.A., Gu, L., Sendinc, E., Liu, J., Aristizabal-Corrales, D., Hsu, C.H., Aravind, L., He, C. and Shi, Y. (2015) DNA Methylation on N6-Adenine in C. elegans. *Cell*, **161**, 868-878.

7. Mondo, S.J., Dannebaum, R.O., Kuo, R.C., Louie, K.B., Bewick, A.J., LaButti, K., Haridas, S., Kuo, A., Salamov, A., Ahrendt, S.R. *et al.* (2017) Widespread adenine N6-methylation of active genes in fungi. *Nat Genet*, **49**, 964-968.

8. Blow, M.J., Clark, T.A., Daum, C.G., Deutschbauer, A.M., Fomenkov, A., Fries, R., Froula, J., Kang, D.D., Malmstrom, R.R., Morgan, R.D. *et al.* (2016) The Epigenomic Landscape of Prokaryotes. *PLoS Genet*, **12**, e1005854.

9. Jeltsch, A. (2002) Beyond Watson and Crick: DNA methylation and molecular enzymology of DNA methyltransferases. *Chembiochem*, **3**, 274-293.

10. Loenen, W.A., Dryden, D.T., Raleigh, E.A. and Wilson, G.G. (2014) Type I restriction enzymes and their relatives. *Nucleic Acids Res*, **42**, 20-44.

11. Loenen, W.A., Dryden, D.T., Raleigh, E.A., Wilson, G.G. and Murray, N.E. (2014) Highlights of the DNA cutters: a short history of the restriction enzymes. *Nucleic Acids Res*, **42**, 3-19.

12. Arber, W. and Dussoix, D. (1962) Host specificity of DNA produced by Escherichia coli. I. Host controlled modification of bacteriophage lambda. *J Mol Biol*, **5**, 18-36.

13. Gold, M., Hurwitz, J. and Anders, M. (1963) The Enzymatic Methylation of Rna and DNA, Ii. On the Species Specificity of the Methylation Enzymes. *Proc Natl Acad Sci U S A*, **50**, 164-169.

14. Cheng, X. (1995) DNA modification by methyltransferases. *Curr Opin Struct Biol*, **5**, 4-10.

15. Seshasayee, A.S., Singh, P. and Krishna, S. (2012) Context-dependent conservation of DNA methyltransferases in bacteria. *Nucleic Acids Res*, **40**, 7066-7073.

16. Gonzalez, D., Kozdon, J.B., McAdams, H.H., Shapiro, L. and Collier, J. (2014) The functions of DNA methylation by CcrM in Caulobacter crescentus: a global approach. *Nucleic Acids Res*, **42**, 3720-3735.

17. Han, J.S., Kang, S., Kim, S.H., Ko, M.J. and Hwang, D.S. (2004) Binding of SeqA protein to hemi-methylated GATC sequences enhances their interaction and aggregation properties. *J Biol Chem*, **279**, 30236-30243.

18. Nievera, C., Torgue, J.J., Grimwade, J.E. and Leonard, A.C. (2006) SeqA blocking of DnaA-oriC interactions ensures staged assembly of the E. coli pre-RC. *Mol Cell*, **24**, 581-592.

19. Lahue, R.S., Au, K.G. and Modrich, P. (1989) DNA mismatch correction in a defined system. *Science*, **245**, 160-164.

20. Bale, A., d'Alarcao, M. and Marinus, M.G. (1979) Characterization of DNA adenine methylation mutants of Escherichia coli K12. *Mutat Res*, **59**, 157-165.

21. Pukkila, P.J., Peterson, J., Herman, G., Modrich, P. and Meselson, M. (1983) Effects of high levels of DNA adenine methylation on methyl-directed mismatch repair in Escherichia coli. *Genetics*, **104**, 571-582.

22. Casadesus, J. and Low, D.A. (2013) Programmed heterogeneity: epigenetic mechanisms in bacteria. *J Biol Chem*, **288**, 13929-13935.

23. Atack, J.M., Yang, Y., Seib, K.L., Zhou, Y. and Jennings, M.P. (2018) A survey of Type III restriction-modification systems reveals numerous, novel epigenetic regulators controlling phase-variable regulons; phasevarions. *Nucleic Acids Res*, **46**, 3532-3542.

24. Hernday, A.D., Braaten, B.A. and Low, D.A. (2003) The mechanism by which DNA adenine methylase and PapI activate the pap epigenetic switch. *Mol Cell*, **12**, 947-957.

25. Seib, K.L., Jen, F.E., Tan, A., Scott, A.L., Kumar, R., Power, P.M., Chen, L.T., Wu, H.J., Wang, A.H., Hill, D.M. *et al.* (2015) Specificity of the ModA11, ModA12 and ModD1 epigenetic regulator N(6)-adenine DNA methyltransferases of Neisseria meningitidis. *Nucleic Acids Res*, **43**, 4150-4162.

26. Nye, T.M., Jacob, K.M., Holley, E.K., Nevarez, J.M., Dawid, S., Simmons, L.A. and Watson, M.E., Jr. (2019) DNA methylation from a Type I restriction modification system influences gene expression and virulence in Streptococcus pyogenes. *PLoS Pathog*, **15**, e1007841.

27. Wojciechowski, M., Czapinska, H. and Bochtler, M. (2013) CpG underrepresentation and the bacterial CpG-specific DNA methyltransferase M.MpeI. *Proc Natl Acad Sci U S A*, **110**, 105-110.

28. Eid, J., Fehr, A., Gray, J., Luong, K., Lyle, J., Otto, G., Peluso, P., Rank, D., Baybayan, P., Bettman, B. *et al.* (2009) Real-time DNA sequencing from single polymerase molecules. *Science*, **323**, 133-138.

29. Flusberg, B.A., Webster, D.R., Lee, J.H., Travers, K.J., Olivares, E.C., Clark, T.A., Korlach, J. and Turner, S.W. (2010) Direct detection of DNA methylation during single-molecule, real-time sequencing. *Nat Methods*, **7**, 461-465.

30. Wion, D. and Casadesus, J. (2006) N6-methyl-adenine: an epigenetic signal for DNA-protein interactions. *Nat Rev Microbiol*, **4**, 183-192.

31. Bolker, M. and Kahmann, R. (1989) The Escherichia coli regulatory protein OxyR discriminates between methylated and unmethylated states of the phage Mu mom promoter. *EMBO J*, **8**, 2403-2410.

32. Nou, X., Skinner, B., Braaten, B., Blyn, L., Hirsch, D. and Low, D. (1993) Regulation of pyelonephritis-associated pili phase-variation in Escherichia coli: binding of the PapI and the Lrp regulatory proteins is controlled by DNA methylation. *Mol Microbiol*, **7**, 545-553.

33. Ogawa, T. and Okazaki, T. (1994) Cell cycle-dependent transcription from the gid and mioC promoters of Escherichia coli. *J Bacteriol*, **176**, 1609-1615.

34. Lobner-Olesen, A., Marinus, M.G. and Hansen, F.G. (2003) Role of SeqA and Dam in Escherichia coli gene expression: a global/microarray analysis. *Proc Natl Acad Sci U S A*, **100**, 4672-4677.

35. Lu, M., Campbell, J.L., Boye, E. and Kleckner, N. (1994) SeqA: a negative modulator of replication initiation in E. coli. *Cell*, **77**, 413-426.

36. Marinus, M.G. and Morris, N.R. (1975) Pleiotropic effects of a DNA adenine methylation mutation (dam-3) in Escherichia coli K12. *Mutat Res*, **28**, 15-26.

37. Stephens, C., Reisenauer, A., Wright, R. and Shapiro, L. (1996) A cell cycle-regulated bacterial DNA methyltransferase is essential for viability. *Proc Natl Acad Sci U S A*, **93**, 1210-1214.

38. Koo, B.M., Kritikos, G., Farelli, J.D., Todor, H., Tong, K., Kimsey, H., Wapinski, I., Galardini, M., Cabal, A., Peters, J.M. *et al.* (2017) Construction and Analysis of Two Genome-Scale Deletion Libraries for Bacillus subtilis. *Cell Syst*, **4**, 291-305 e297.

39. Hardwood, C.R. and Cutting, S.M. (1990) *Molecular Biological Methods for Bacillus*. John Wiley Sons, Chichester.

40. Nye, T.M., Schroeder, J.W., Kearns, D.B. and Simmons, L.A. (2017) Complete Genome Sequence of Undomesticated Bacillus subtilis Strain NCIB 3610. *Genome Announc*, **5**, pii: e00364-00317.

41. Schroeder, J.W. and Simmons, L.A. (2013) Complete Genome Sequence of Bacillus subtilis Strain PY79. *Genome Announcements*, **1**, pii: e01085-01013.

42. Sobetzko, P., Jelonek, L., Strickert, M., Han, W., Goesmann, A. and Waldminghaus, T. (2016) DistAMo: A Web-Based Tool to Characterize DNA-Motif Distribution on Bacterial Chromosomes. *Front Microbiol*, **7**, 283.

43. Zwietering, M.H., Jongenburger, I., Rombouts, F.M. and van 't Riet, K. (1990) Modeling of the bacterial growth curve. *Appl Environ Microbiol*, **56**, 1875-1881.

44. Dreiseikelmann, B. and Wackernagel, W. (1981) Absence in Bacillus subtilis and Staphylococcus aureus of the sequence-specific deoxyribonucleic acid methylation that is conferred in Escherichia coli K-12 by the dam and dcm enzymes. *J Bacteriol*, **147**, 259-261.

45. Guha, S. and Guschlbauer, W. (1992) Expression of Escherichia coli dam gene in Bacillus subtilis provokes DNA damage response: N6-methyladenine is removed by two repair pathways. *Nucleic Acids Res*, **20**, 3607-3615.

46. Kearns, D.B., Chu, F., Rudner, R. and Losick, R. (2004) Genes governing swarming in Bacillus subtilis and evidence for a phase variation mechanism controlling surface motility. *Mol Microbiol*, **52**, 357-369.

47. Ohshima, H., Matsuoka, S., Asai, K. and Sadaie, Y. (2002) Molecular organization of intrinsic restriction and modification genes BsuM of Bacillus subtilis Marburg. *J Bacteriol*, **184**, 381-389.

48. Schluckebier, G., O'Gara, M., Saenger, W. and Cheng, X. (1995) Universal catalytic domain structure of AdoMet-dependent methyltransferases. *J Mol Biol*, **247**, 16-20.

49. Morgan, R.D., Dwinell, E.A., Bhatia, T.K., Lang, E.M. and Luyten, Y.A. (2009) The MmeI family: type II restriction-modification enzymes that employ single-strand modification for host protection. *Nucleic Acids Res*, **37**, 5208-5221.

50. Sanchez-Romero, M.A., Cota, I. and Casadesus, J. (2015) DNA methylation in bacteria: from the methyl group to the methylome. *Curr Opin Microbiol*, **25**, 9-16.

51. Nicolas, P., Mader, U., Dervyn, E., Rochat, T., Leduc, A., Pigeonneau, N., Bidnenko, E., Marchadier, E., Hoebeke, M., Aymerich, S. *et al.* (2012) Condition-dependent transcriptome reveals high-level regulatory architecture in Bacillus subtilis. *Science*, **335**, 1103-1106.

52. Voelker, U., Luo, T., Smirnova, N. and Haldenwang, W. (1997) Stress activation of Bacillus subtilis sigma B can occur in the absence of the sigma B negative regulator RsbX. *J Bacteriol*, **179**, 1980-1984.

53. Gueiros-Filho, F.J. and Losick, R. (2002) A widely conserved bacterial cell division protein that promotes assembly of the tubulin-like protein FtsZ. *Genes Dev*, **16**, 2544-2556.

54. Seo, D., Kamino, K., Inoue, K. and Sakurai, H. (2004) Purification and characterization of ferredoxin-NADP+ reductase encoded by Bacillus subtilis yumC. *Arch Microbiol*, **182**, 80-89.

55. Mascarenhas, J., Soppa, J., Strunnikov, A.V. and Graumann, P.L. (2002) Cell cycle-dependent localization of two novel prokaryotic chromosome segregation and condensation proteins in Bacillus subtilis that interact with SMC protein. *Embo J*, **21**, 3108-3118.

56. Wang, X., Le, T.B., Lajoie, B.R., Dekker, J., Laub, M.T. and Rudner, D.Z. (2015) Condensin promotes the juxtaposition of DNA flanking its loading site in Bacillus subtilis. *Genes Dev*, **29**, 1661-1675.

57. Wang, X., Montero Llopis, P. and Rudner, D.Z. (2014) Bacillus subtilis chromosome organization oscillates between two distinct patterns. *Proc Natl Acad Sci U S A*, **111**, 12877-12882.

58. Wang, X., Tang, O.W., Riley, E.P. and Rudner, D.Z. (2014) The SMC condensin complex is required for origin segregation in Bacillus subtilis. *Curr Biol*, **24**, 287-292.

59. Carabetta, V.J., Greco, T.M., Cristea, I.M. and Dubnau, D. (2019) YfmK is an N(epsilon)-lysine acetyltransferase that directly acetylates the histone-like protein HBsu in Bacillus subtilis. *Proc Natl Acad Sci U S A*, **116**, 3752-3757.

60. Kohler, P. and Marahiel, M.A. (1998) Mutational analysis of the nucleoid-associated protein HBsu of Bacillus subtilis. *Mol Gen Genet*, **260**, 487-491.

61. Lalanne, J.B., Taggart, J.C., Guo, M.S., Herzel, L., Schieler, A. and Li, G.W. (2018) Evolutionary Convergence of Pathway-Specific Enzyme Expression Stoichiometry. *Cell*, **173**, 749-761 e738.

62. Randall, J.R., Hirst, W.G. and Simmons, L.A. (2017) Substrate specificity for bacterial RNase HII and HIII is influenced by metal availability. *J Bacteriol*, **200**, pii: e00401-00417.

63. Randall, J.R., Nye, T.M., Wozniak, K.J. and Simmons, L.A. (2019) RNase HIII Is Important for Okazaki Fragment Processing in Bacillus subtilis. *J Bacteriol*, **201**, pii: e00686-00618.

64. Stolz, R., Sulthana, S., Hartono, S.R., Malig, M., Benham, C.J. and Chedin, F. (2019) Interplay between DNA sequence and negative superhelicity drives R-loop structures. *Proc Natl Acad Sci U S A*. 116(13):6260-6269.

65. Belitsky, B.R., Barbieri, G., Albertini, A.M., Ferrari, E., Strauch, M.A. and Sonenshein, A.L. (2015) Interactive regulation by the Bacillus subtilis global regulators CodY and ScoC. *Mol Microbiol*, **97**, 698-716.

66. Caldwell, R., Sapolsky, R., Weyler, W., Maile, R.R., Causey, S.C. and Ferrari, E. (2001) Correlation between Bacillus subtilis scoC phenotype and gene expression determined using microarrays for transcriptome analysis. *J Bacteriol*, **183**, 7329-7340.

67. Marinus, M.G. and Lobner-Olesen, A. (2014) DNA Methylation. *EcoSal Plus*, **6**, doi: 10.1128/ecosalplus.ESP-0003-2013.

68. Kozdon, J.B., Melfi, M.D., Luong, K., Clark, T.A., Boitano, M., Wang, S., Zhou, B., Gonzalez, D., Collier, J., Turner, S.W. *et al.* (2013) Global methylation state at base-pair resolution of the Caulobacter genome throughout the cell cycle. *Proc Natl Acad Sci U S A*, **110**, E4658-4667.

69. Casadesus, J. and Low, D. (2006) Epigenetic gene regulation in the bacterial world. *Microbiol Mol Biol Rev*, **70**, 830-856.

70. Waldron, D.E., Owen, P. and Dorman, C.J. (2002) Competitive interaction of the OxyR DNA-binding protein and the Dam methylase at the antigen 43 gene regulatory region in Escherichia coli. *Mol Microbiol*, **44**, 509-520.

71. Haakonsen, D.L., Yuan, A.H. and Laub, M.T. (2015) The bacterial cell cycle regulator GcrA is a sigma70 cofactor that drives gene expression from a subset of methylated promoters. *Genes Dev*, **29**, 2272-2286.

72. Jarmer, H., Larsen, T.S., Krogh, A., Saxild, H.H., Brunak, S. and Knudsen, S. (2001) Sigma A recognition sites in the Bacillus subtilis genome. *Microbiology*, **147**, 2417-2424.

73. Diekmann, S. (1987) DNA methylation can enhance or induce DNA curvature. *EMBO J*, **6**, 4213-4217.

74. Camacho, E.M., Serna, A., Madrid, C., Marques, S., Fernandez, R., de la Cruz, F., Juarez, A. and Casadesus, J. (2005) Regulation of finP transcription by DNA adenine methylation in the virulence plasmid of Salmonella enterica. *J Bacteriol*, **187**, 5691-5699.

Figure Legends

Figure 1. Motif enrichment analysis for m6A sites in the *B. subtilis* PY79 chromosome. Motif enrichment analysis was performed using the DistAMo web based server tool (42). Sliding windows of 50 kb to 500 kb are represented by the rings from outside (large) to inside (small) rings scaling in 50 kb increment increases. Over (red) and under (blue) enrichment are represented by z-scores in the scale indicated. **(A)** m6A motif enrichment for all motifs with *ori* and *ter* regions indicated; **(B)** m6A motif enrichment on the leading strand; **(C)** m6A motif enrichment on the lagging strand.

Figure 2. DnmA is sufficient for methylation of dsDNA at 5'GACGAG sites. **(A)** SDS-polyacrylamide gel of purified catalytically inactive DnmA variant Y465A, WT DnmA (M.BsuPY79I), and YabB. (*) indicates DnmA multimer. **(B)** DnmA (M.BsuPY79I) incorporation of tritiated SAM into dsDNA and ssDNA substrates carrying the GACGAG sequence over time. Y465A (indicated in blue) is a DnmA (M.BsuPY79I) catalytically inactive variant. **(C)** Incorporation of tritiated SAM into DNA and RNA substrates by uncharacterized MTases DnmA (M.BsuPY79I) and YabB. **(D)** DnmA (M.BsuPY79I) incorporation of tritiated SAM onto indicated substrates. The DnmA catalytically inactive variant is indicated.

Figure 3. Loss of DnmA does not affect growth rate or transformation efficiency of foreign methylated DNA. (A) Growth curves for WT, Δ*dnmA,* Δ*yabB,* and Δ*dnmA*Δ*yabB* were performed in triplicate and fit to a Gompertz growth model (43) to calculate growth rate. Growth rate and the corresponding 95% confidence interval for each strain are indicated. **(B)** Plasmid map of pHP13 with the location of each m6A site

shown. The orange carrots indicate the relative position and strand orientation for each site. **(C)** Transformation efficiency assays were performed using pHP13 plasmid purified from *E. coli* as donor DNA in WT, Δ*dnmA,* Δ*rok,* and Δ*comK* recipient strains. The average transformation efficiency and standard error for each strain is indicated.

Figure 4. Methylation of DnmA motifs in proximity of -35 boxes affects downstream gene expression. **(A)** Schematic overview of the promoter regions containing DnmA sites that were selected for analysis using transcriptional GFP fusions. Indicated are the locations of the predicted sigma factor -35 and -10 boxes with respect to the DnmA motifs. U numbers correspond to the transcribed regions 5' of ORFs identified by Nicolas *et al* (51). **(B)** The location of the studied promoters on the PY79 chromosome map with respect to the *amyE* site used for integration and analysis of the promoter-GFP constructs. **(C)** Histograms depicting the GFP fluorescence in 200,000 WT (blue) or Δ*dnmA* (red) cells in three biological replicates that were grown in $S7_{50}$ medium to an OD_{600} of 0.5 at 30°C and measured using flow cytometry. For U0374/P_{sigB}, an additional experiment was performed in which the cells were treated with 4% EtOH an hour before analysis with flow cytometry. The standard deviations are represented as shaded areas. Promoter regions that appear methylation sensitive are shown in green. **(D)** Scatter dot plots, with indicated mean and standard deviation, depicting the median fluorescence of each strain taken from the histograms shown in (C) and appended with similar measurements taken on at least one different day. A standard T-test was performed to evaluate differential GFP expression between WT and Δ*dnmA* for each promoter. *p*-values: * = $p < 0.05$, *** = $p < 0.005$, **** = $p < 0.001$.

Figure 5. Mutating the DnmA recognition motif is sufficient for differential gene expression in the *PscpA* promoter. (A) Analysis of the effect of mutating WT GACG**A**G to GACG**C**G (first graph), GACG**T**G (second graph), or GACGA**C** (third

graph) on the activity of P*scpA*-GFP in WT (teal) and Δ*dnmA* (orange) cells. **(B)** Scatter dot plots, with indicated mean and standard deviation, of the median GFP fluorescence of each strain taken from the histograms shown in (A) and appended with measurements from a similar experiment taken on a separate day. The median values were tested against each other, including the median values from the strain expressing P*scpA*-GFP in WT cells, for differential expression using a one-way ANOVA post-hoc Tuckey test. *p*-values: * = $p < 0.05$, *** = $p < 0.005$, **** = $p < 0.001$, ns = not significant.

Figure 6. Transcription factor ScoC binds the *scpA* promoter with an unmodified GACGAG site. (A) Top protein hits identified in the pull-down of the biotinylated *scpA* promoter regions with GACGAG and GACGTG sites. The #PSMs indicates the total number of peptide spectra identified for each protein using the indicated oligo in the lysate pull-down assay. **(B)** SDS-polyacrylamide gel of ScoC overexpressed and purified from *E. coli* and stained with Coomassie. **(C)** Schematic of the *scpA* promoter region. The ScoC binding consensus sequence is shown in blue, the m6A site is in red, and the -35 box is also indicated. **(D)** ScoC binding to 5' IR dye end-labeled *scpA* promoter region containing a GACGAG or GACGTG site was determined via EMSA. Representative electrophoretic mobility shift assay (EMSA) of ScoC binding to *scpA* promoter regions is shown. The concentration of ScoC is shown with (-) indicating the absence of ScoC from the reaction. Oligos containing the GACGAG or GACGTG site are also indicated at the top of the gel. The DNA substrates used in the reaction are otherwise identical. **(E)** Quantification of the percent band shifted using 250 nM and 500 nM concentrations of ScoC for the GACGAG and GACGTG oligos as indicated on the graph. The percent band shifted was normalized to the no protein control for each substrate. Three replicates were completed with the error bars representing the standard error between reactions.

Table 1. Relevant modified motifs detected in *B. subtilis* by PacBio SMRT sequencing.

Motif[a]	Type	%Detected	Mean QV	Mean Cov.	Mean IPD Ratio
WT PY79					
GACG**A**G	m6A	99.7	388	286	6.72
CTCGARB	m5C[b]	70.8	74	270	1.89
WT 3610					
GACG**A**G	m6A	94.7	362	313	4.84

[a]All motif calls by SMRT sequencing are reported in Supplementary Table S4.
[b]Modification type confirmed via methylation sensitive restriction endonuclease digest as described in the supporting document.

Table 2. Relevant modified motifs detected in *B. subtilis* by PacBio SMRT sequencing.

Motif[a]	Type	%Detected	Mean QV	Mean Cov.	Mean IPD Ratio
Δ*dnmA* WT PY79					
CTCGARB	m5C[b]	46.7	51	120	2.00
Δ*dnmA* WT 3610					
None[c]				358	
Δ*dnmA, amyE::Pspac dnmA* PY79					
GACG**A**G	m6A	99.7	213	152	6.32
CTCGARB	m5C	52.7	59	149	2.00

[a]All motif calls by SMRT sequencing are reported in Supplementary Table S6.
[b]Modification type confirmed via methylation sensitive restriction endonuclease treatment as described in the supporting document.
[c]GACGAG and CTCGARB were not detected in NCIB 3610 Δ*dnmA*. All other motifs called are reported in Supplementary Table S6. The average coverage is reported for each spurious motif detected.

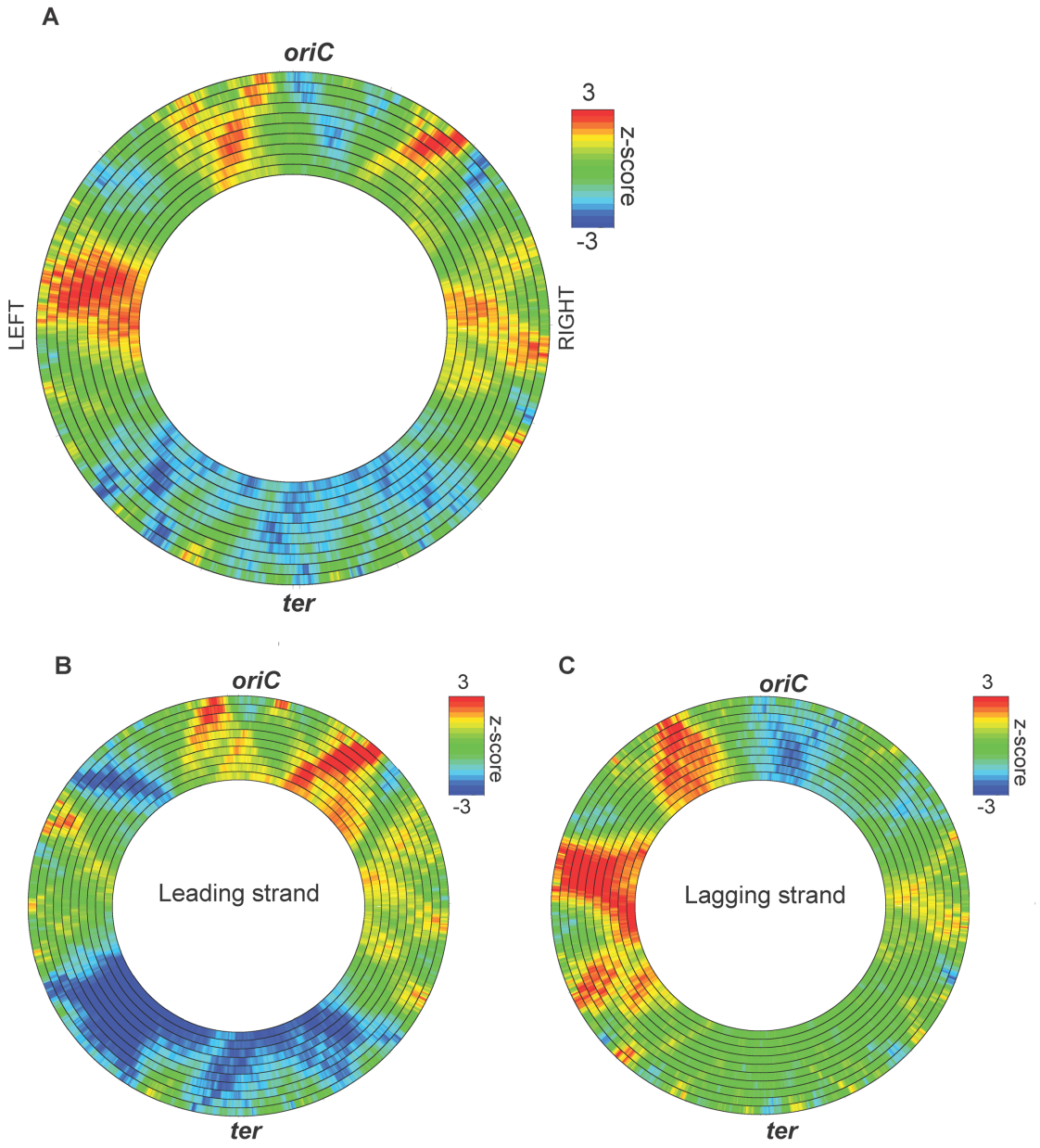
A
oriC
3
z-score
-3
LEFT
RIGHT
ter
B
oriC
3
z-score
-3
Leading strand
ter
C
oriC
3
z-score
-3
Lagging strand
ter

Figure 1.

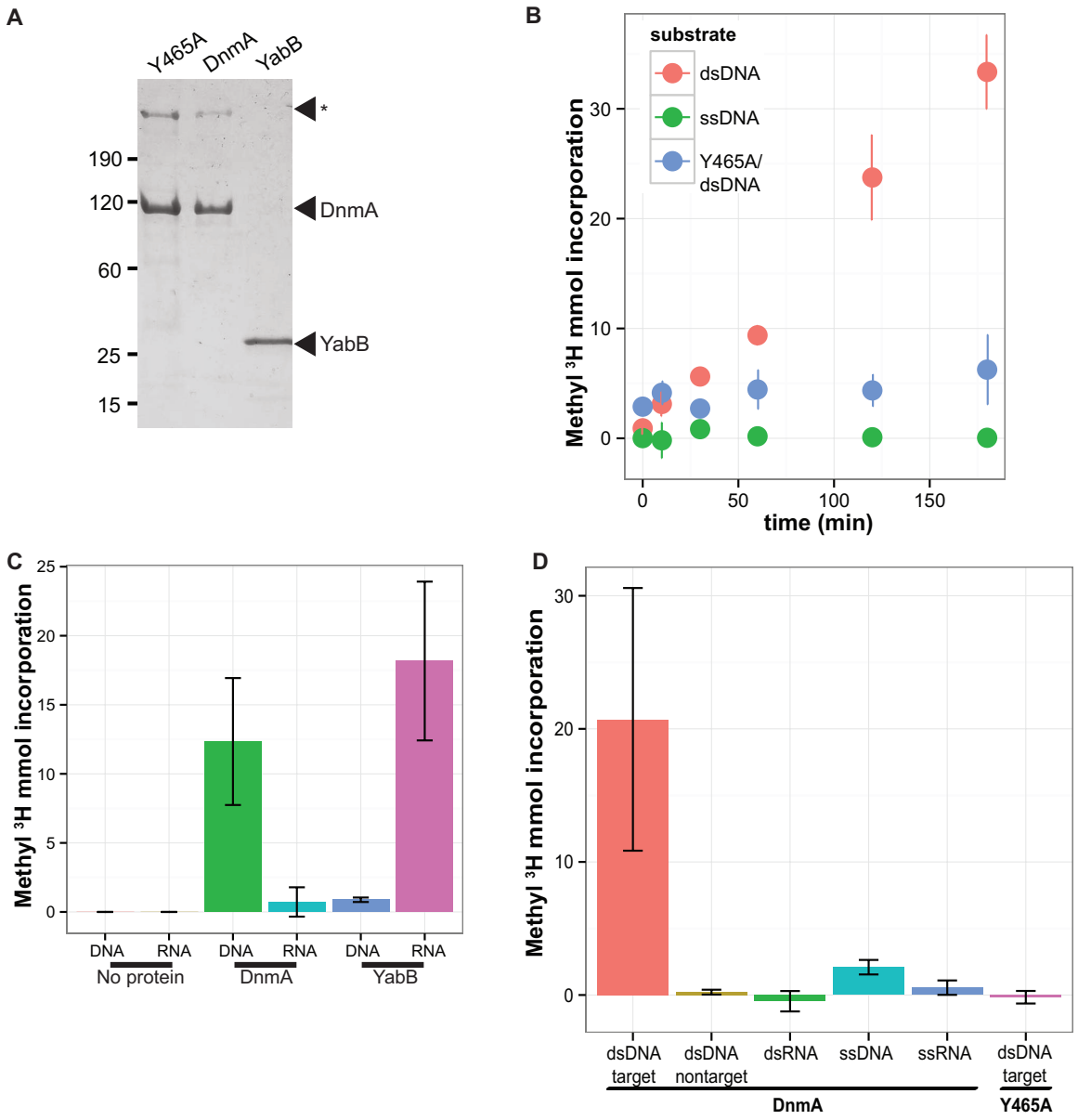
A
Y465A
DnmA
YabB
190
120
60
25
15
*
DnmA
YabB
B
substrate
dsDNA
ssDNA
Y465A/
dsDNA
Methyl ³H mmol incorporation
time (min)
C
Methyl ³H mmol incorporation
DNA
RNA
No protein
DnmA
YabB
D
Methyl ³H mmol incorporation
dsDNA target
dsDNA nontarget
dsRNA
ssDNA
ssRNA
dsDNA target
DnmA
Y465A

Figure 2.

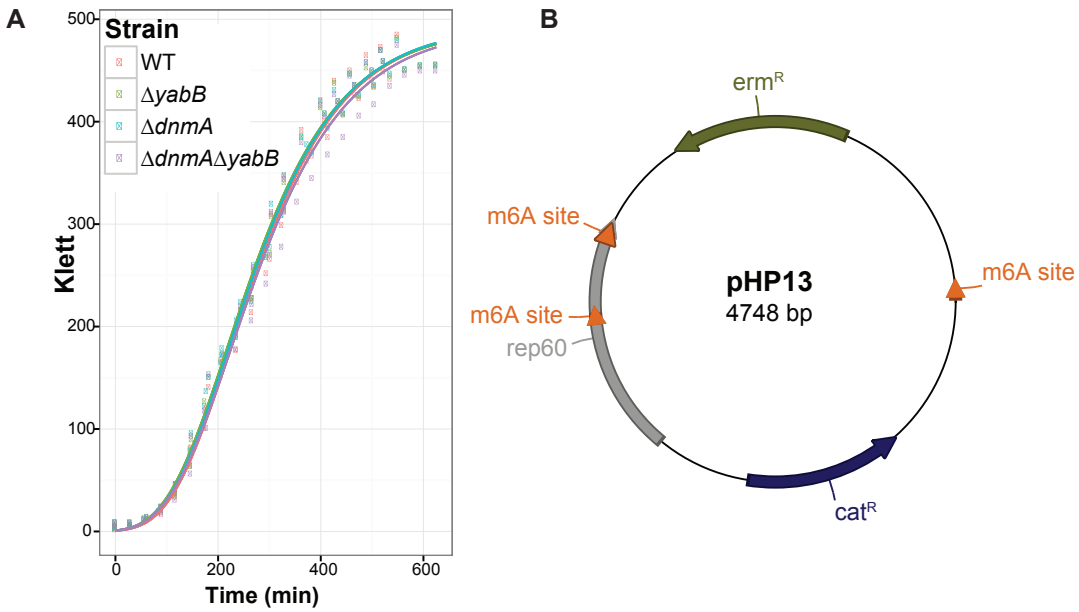

Relevant genotype	Growth rate	95% CI
Wild type	1.52	[1.43, 1.61]
Δ*dnmA*	1.51	[1.43, 1.59]
Δ*yabB*	1.51	[1.43-1.58]
Δ*dnmA*Δ*yabB*	1.46	[1.35-1.57]

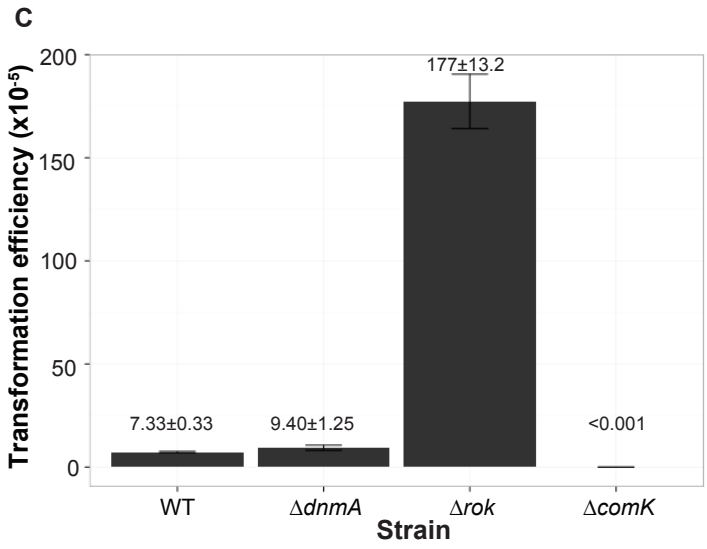

Figure 3.

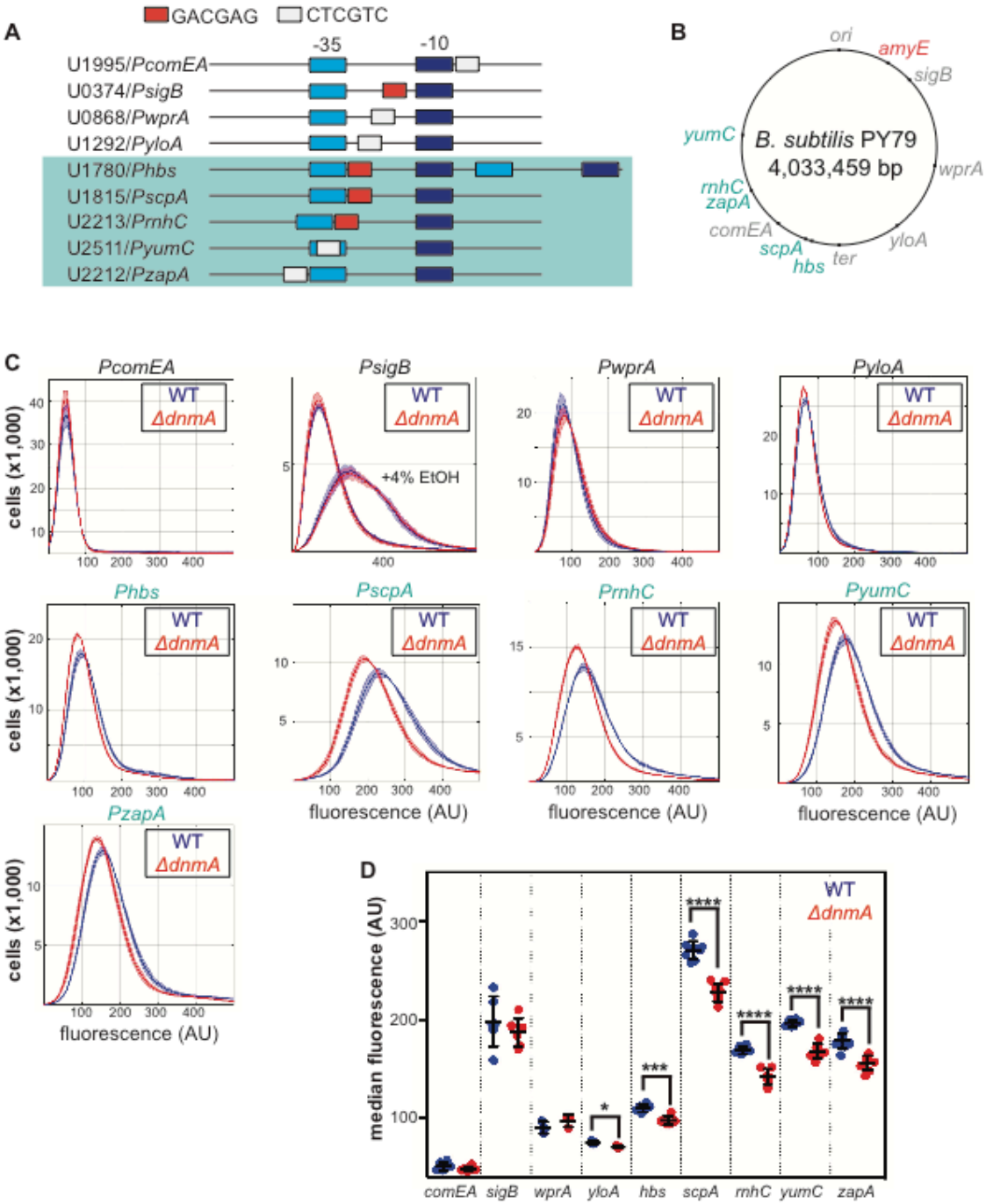
A
GACGAG
CTCGTC
-35
-10
U1995/PcomEA
U0374/PsigB
U0868/PwprA
U1292/PyloA
U1780/Phbs
U1815/PscpA
U2213/PrnhC
U2511/PyumC
U2212/PzapA
B
ori
amyE
sigB
yumC
B. subtilis PY79
4,033,459 bp
wprA
rnhC
zapA
comEA
scpA
hbs
ter
yloA
C
PcomEA
PsigB
PwprA
PyloA
Phbs
PscpA
PrnhC
PyumC
PzapA
WT
ΔdnmA
+4% EtOH
cells (x1,000)
fluorescence (AU)
D
median fluorescence (AU)
comEA
sigB
wprA
yloA
hbs
scpA
rnhC
yumC
zapA

Figure 4.

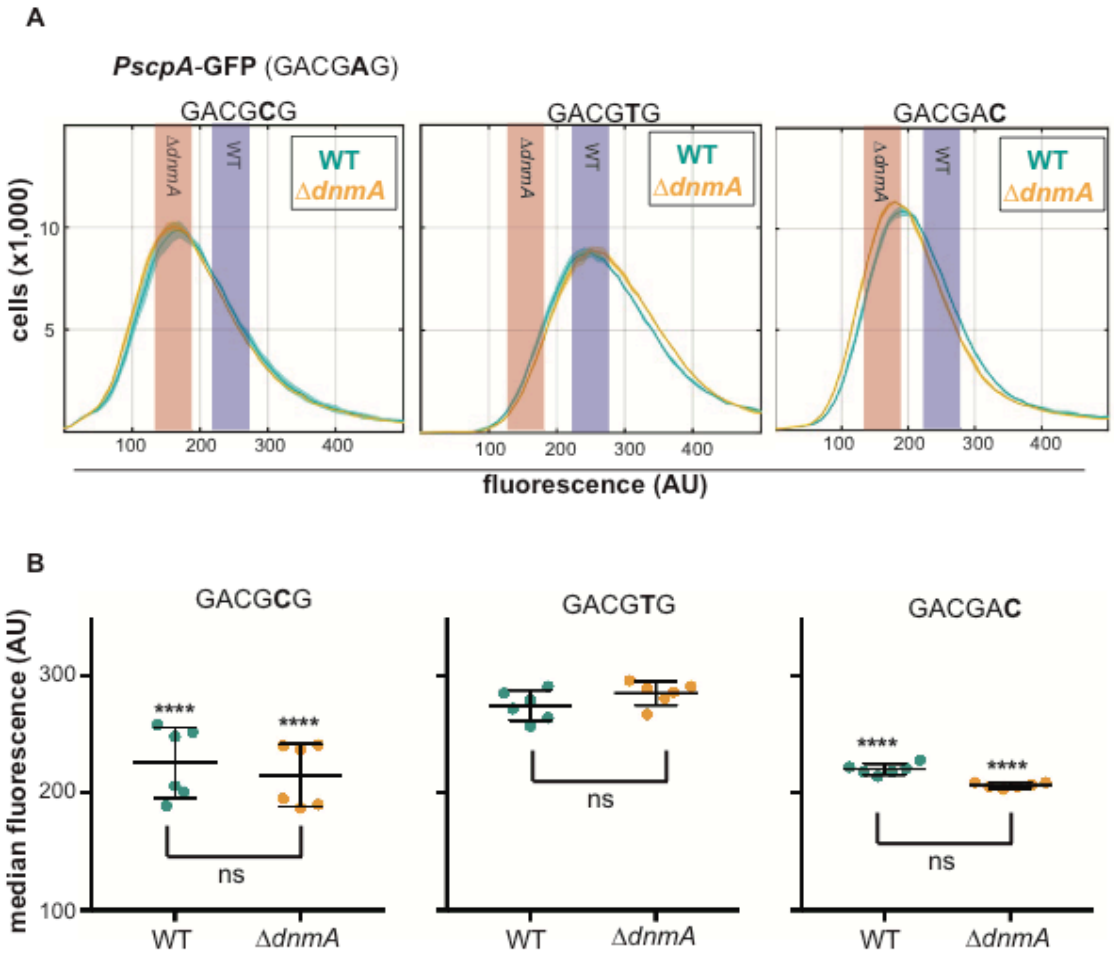
A
PscpA-GFP (GACGAG)
GACGCG
GACGTG
GACGAC
ΔdnmA
WT
WT
ΔdnmA
cells (x1,000)
10
5
100
200
300
400
fluorescence (AU)
B
median fluorescence (AU)
300
200
100
****
ns
WT
ΔdnmA

Figure 5.

A

Protein	Function	MW [kDa]	# PSMs GACGAG	# PSMs GACGTG
FabL	Enoyl-acyl carrier protein reductase	27.2	105	110
RpsE	Ribosomal protein	17.6	29	22
RpsG	Ribosomal protein	17.9	23	11
ScoC	Transcriptional regulator of transition state	23.7	16	0

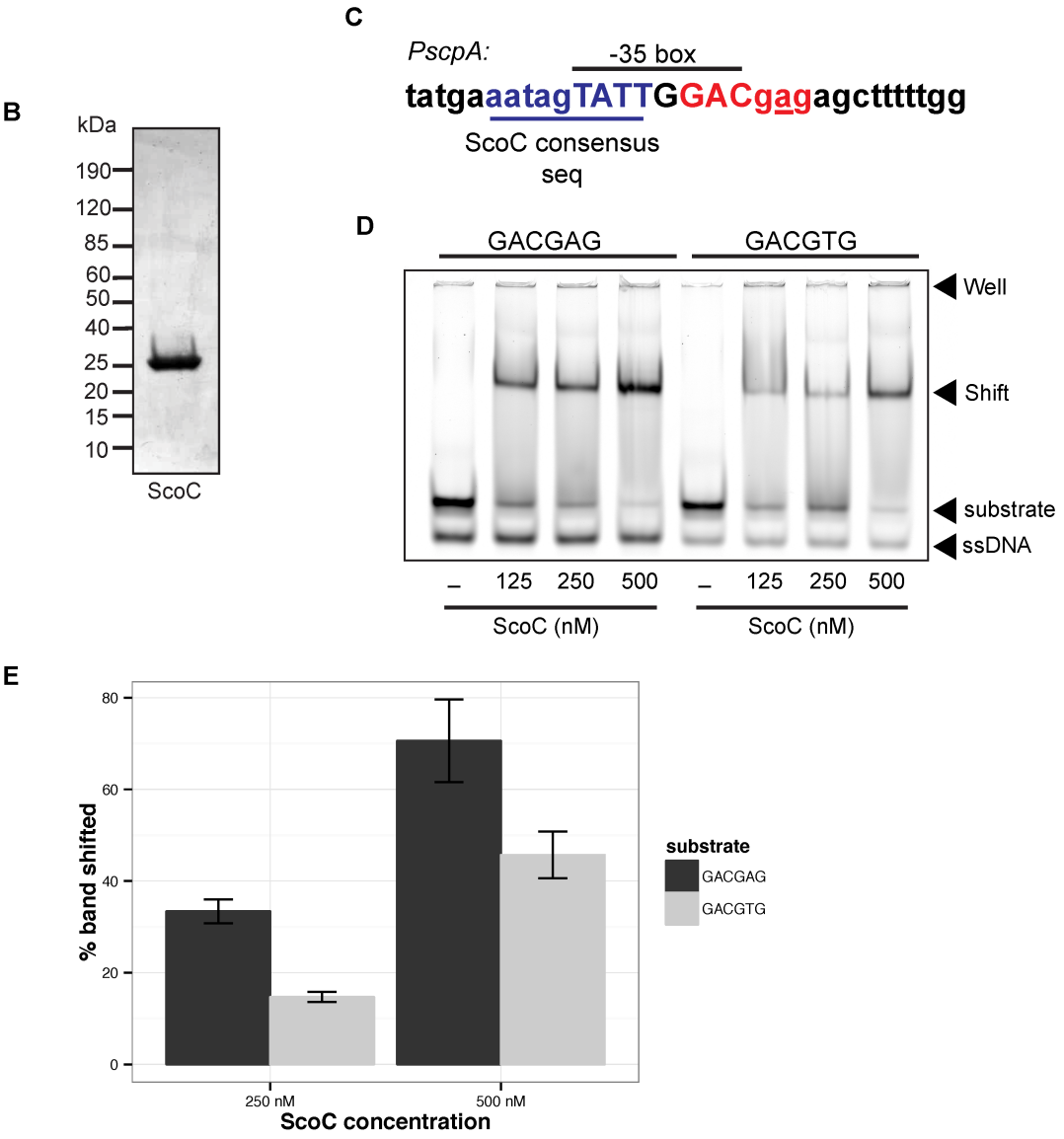

Figure 6.

Supplementary Information

Methyltransferase DnmA is responsible for genome-wide N6-methyladenosine modifications at non-palindromic recognition sites in *Bacillus subtilis*

Taylor M. Nye, Lieke A. van Gijtenbeek, Amanda G. Stevens, Jeremy W. Schroeder, Justin R. Randall, Lindsay A. Matthews, Lyle A. Simmons*

Department of Molecular, Cellular, and Developmental Biology
University of Michigan, Ann Arbor, Michigan USA.

*To whom correspondence should be addressed: Department of Molecular, Cellular, and Developmental Biology, University of Michigan, Ann Arbor, Michigan 48109-1055, United States. Phone: (734) 647-2016, Fax: (734) 615-6337
E-mail: lasimm@umich.edu

Running Title: *Bacillus subtilis* m6A affects gene expression
Keywords: DNA methyltransferase, gene expression, *Bacillus subtilis,* SMRT sequencing, SigA

Supplementary Materials and Methods

Chromosomal DNA digestion by MspJI: Genomic DNA was purified from PY79, Δ*dnmA*, Δ*ydiOP*Δ*ydiR*, Δ*ydiOP*Δ*ydiS*, and Δ*ydiOP*Δ*ydjA* strains as described above and treated for six hours with MspJI according to the manufacturer's recommendations (New England BioLabs). For each control the reaction was set up exactly like the experimental group with an equivalent amount of water added instead of MspJI. Each reaction was then loaded on a 0.7% agarose gel and electrophoresed, stained with ethidium bromide, and visualized by illumination with UV.

DnmA (M.BsuPY79I) Y465A: A PCR reaction was performed using specially designed primers to create two overlapping blocks of DNA coding for *dnmA* with an alanine in the place of the tyrosine usually found in the NPPY catalytic motif. The 5' block was created by PCR using oTMN5 and oAS1 with *B. subtilis* genomic DNA as the template. The 3' block was created by PCR using oAS2 and oTMN7 with *B. subtilis* genomic DNA as the template. PCR products were gel extracted, purified, and combined with pE-SUMO vector via Gibson assembly to create pAS2. The resulting plasmid was used to transform *E. coli* MC1061 cells and plated on LB agar containing 25 µg/ml kanamycin. Resulting colonies were PCR screened for presence of the *dnmA* gene using oTMN5 and oTMN7 and further verified by Sanger sequencing. $BL21_{DE3}$ cells containing this plasmid were then tested for their ability to overexpress the mutant protein with addition of 200 µM IPTG.

Electrophoretic Mobile Shift Assay (EMSA): EMSAs were performed using 1 µM DnmA and 5' IR dye labeled substrates at 0.62 µM in a buffer containing 100 mM Tris-HCl pH 8, 250 mM NaCl, and 1 mM $MgSO_4$. The substrates were annealed in the same buffer by heating to 100°C for 30 seconds and then allowed to cool back to room

temperature on the bench top. Substrates included the target sequence (oAS09, oTMN39), non-target (oAS10, oTMN41), and a degenerate sequence (oAS11, oJR269). A no protein control was used for each substrate and catalytically inactive DnmA (Y465A) was assayed with the target sequence. These assays were performed at 30°C for 15 minutes. Samples were then loaded onto, and resolved via 6% native-PAGE electrophoresed on ice at 100V and visualized with a LI-COR Odyssey imager.

Spot titer assays: The indicated strains were struck from frozen stocks onto LB agar plates and incubated overnight at 30°C. Single colonies were inoculated into 2 mL of LB media and grown in a rolling rack at 37°C to an OD_{600} of 0.6-0.8. Strains were then diluted to an OD_{600} of 0.5 and subsequent 10-fold serial dilutions were performed in 0.85% saline solution. The dilutions (4 µL) were then spotted on LB agar and LB agar plus the indicated concentrations of exogenous DNA damaging agent or HU. Spots were allowed to dry, and the plates were incubated at 30°C overnight.

Mass Spectrometry: Mass spectrometry was performed by The University of Michigan Proteomics & Peptide Synthesis Core, project number MS976/M1516-086. Briefly, the band of interest was excised from SDS-PAGE and placed in 50 µl of distilled water. The band was then digested with trypsin and analyzed using LC/MS/MS on a ThermoFisher Orbitrap mass spectrometer. Resulting data was searched against the NCBI protein database and presented in Supplementary Table S10.

Spontaneous mutagenesis assay: Protocol was followed essentially as described (1). Briefly, frozen strains were struck out on LB and grown at 30°C overnight. Single colonies were inoculated into 3 mL of LB media and grow at 37°C to an OD_{600} between 1 and 1.2. At this point, 1.5 mL of culture was pelleted by centrifugation and the supernatant was aspirated. Cells were resuspended in 0.85% saline and two 1,000-fold

serial dilutions were performed in 0.85% saline. 100 µL of the original solution was plated on LB plates containing 100 µg/mL rifampin and grown at 30°C overnight and 100 µL from the 10^{-6} dilution was plated on LB and grown at 30°C overnight. The number of single colonies on each plate was counted the next morning and mutation rate was calculated using the Ma-Sandri-Sarkar Maximum Likelihood Estimator Method through the FALCOR fluctuation analysis calculator (2). All strains were independently grown and plated on at least three different days.

Live cell microscopy: Protocol was followed essentially as described (3). Frozen strains were struck on LB plates and grown overnight at 37°C. Plates were washed with defined $S7_{50}$ minimal media and diluted back to an OD_{600} of 0.05 in 2 mL of defined $S7_{50}$ minimal media and grown at 37°C to mid-exponential growth phase (OD_{600} between 0.6-0.8). 1 mL aliquots were then treated with 1 µL of FM4-64, the vital membrane strain, and spotted onto 1% agarose pads containing 1X Spizizen's salts. Fluorescence microscopy was performed with an Olympus BX61 microscope. The Olympus 100X oil immersion 1.45 numerical aperture (NA) total internal reflection fluorescence microscopy (TIRFM) objective lens was used for all imaging and all strains were independently imaged on at least three different days.

Strain construction

JWS261 (Δ*ydiOP,* Δ*ydiR*): PY79 was transformed with genomic DNA from BKE06090 to make strain JWS245. JWS245 was transformed with pDR224 to make JWS248. JWS248 was transformed with pJS146.

JWS262 (Δ*ydiOP,* Δ*ydiS*): PY79 was transformed with genomic DNA from BKE06100 to make strain JWS246. JWS246 was transformed with pDR224 to make JWS249. JWS249 was transformed with pJS146.

JWS263 (Δ*ydiOP,* Δ*ydjA*): PY79 was transformed with genomic DNA from BKE06110 to make strain JWS247. JWS247 was transformed with pDR224 to make JWS250. JWS250 was transformed with pJS146.

TMN1 and TMN2 (Δ*yabB)*: PY79 was transformed with genomic DNA from BKE00340 to make strain JWS230. JWS230 was transformed with pDR224.

TMN5 and TMN6 (Δ*dnmA)*: PY79 was transformed with genomic DNA from BKE06760 to make strain JWS230. JWS230 was transformed with pDR224.

TMN16 (Δ*dnmA, amyE::Pspac dnmA*): TMN5 was transformed with pTN003.

TMN47 (Δ*dnmA* in NCIB 3610*)*: DK1042 was transformed with genomic DNA from JWS230. JWS230 was transformed with pDR224.

JWS260 (Δ*dnmA, spo0J::spo0J-gfp*): TMN5 was transformed with genomic DNA from JWS259.

TMN80 (Δ*dnmA, spo0J::spo0J-gfp)*: TMN2 was transformed with genomic DNA from JWS259.

LVG066 (*amyE*::*PrbsV-GFP*): PY79 was transformed with plasmid pLVG1-374.

LVG067 (Δ*dnmA*, *amyE*::*PrbsV-GFP*): TMN06 was transformed with plasmid pLVG1-0374.

LVG068 (*amyE*::*PwprA-GFP*): PY79 was transformed with plasmid pLVG1-0868.

LVG069 (Δ*dnmA*, *amyE*::*PwprA-GFP*): TMN06 was transformed with plasmid pLVG1-0868.

LVG070 (*amyE*::*PyloA-GFP*): PY79 was transformed with plasmid pLVG1-1292.

LVG071 (Δ*dnmA*, *amyE*::*PyloA-GFP*): TMN06 was transformed with plasmid pLVG1-1292.

LVG072 (*amyE*::*PzapA-GFP*): PY79 was transformed with Gibson assembled fragment fLVG-2213.

LVG073 (Δ*dnmA*, *amyE*::*PzapA-GFP*): TMN06 was transformed with Gibson assembled fragment fLVG-2213.

LVG074 (*amyE*::*PrnhC-GFP*): PY79 was transformed with Gibson assembled fragment fLVG-2212.

LVG075 (Δ*dnmA*, *amyE*::*PrnhC-GFP*): TMN06 was transformed with Gibson assembled fragment fLVG-2212.

LVG079 (*amyE*::*PcomEA-GFP*): PY79 was transformed with plasmid pLVG1-1995.

LVG080 (Δ*dnmA*, *amyE*::*PcomEA-GFP*): TMN06 was transformed with plasmid pLVG1-1995.

LVG081 (*amyE*::*PezrA-GFP*): PY79 was transformed with plasmid pLVG1-2292.

LVG082 (Δ*dnmA*, *amyE*::*PezrA-GFP*): TMN06 was transformed with plasmid pLVG1-2292.

LVG087 (*amyE*::*PscpA-GFP*): PY79 was transformed with Gibson assembled fragment fLVG-1815.

LVG088 (Δ*dnmA*, *amyE*::*PscpA-GFP*): TMN06 was transformed with Gibson assembled fragment fLVG-1815.

LVG108 (Δ*dnmA operon*, *amyE*::*PscpA-GFP*): TMN17 was transformed with Gibson assembled fragment fLVG-1815.

LVG102 (*amyE*::*PscpA*^{mut1}*-GFP*): PY79 was transformed with Gibson assembled fragment fLVG-1815mut1.

LVG103 (Δ*dnmA*, *amyE*::*PscpA*^{mut1}*-GFP*): TMN06 was transformed with Gibson assembled fragment fLVG-1815mut1.

LVG109 (Δ*dnmA operon*, *amyE*::*PscpA*^{mut1}*-GFP*): TMN17 was transformed with Gibson assembled fragment fLVG-1815mut1.

LVG105 (*amyE*::*Phbs-GFP*): PY79 was transformed with Gibson assembled fragment fLVG-1780.

LVG106 (Δ*dnmA*, *amyE*::*Phbs-GFP*): TMN06 was transformed with Gibson assembled fragment fLVG-1780.

LVG118 (*amyE*::*PscpA*^{mut2}*-GFP*): PY79 was transformed with Gibson assembled fragment fLVG-1815mut2.

LVG119 (Δ*dnmA operon*, *amyE*::*PscpA*^{mut2}*-GFP*): TMN17 was transformed with Gibson assembled fragment fLVG-1815mut2.

LVG120 (*amyE*::*PscpA*^{mut3}*-GFP*): PY79 was transformed with Gibson assembled fragment fLVG-1815mut3.

LVG121(Δ*dnmA operon*, *amyE*::*PscpA*^{mut3}*-GFP*): TMN17 was transformed with Gibson assembled fragment fLVG-1815mut3.

Plasmid construction

General cloning techniques

All pLVG1-derived plasmids and *amyE*-containing linear fragments were assembled using Gibson assembly (4). Enzymatic assembly of overlapping DNA fragments, or overlap extension PCR. Gibson assemblies consisted of 30-80 ng of each PCR product

and 1X Gibson assembly mastermix (0.1 M Tris pH 8.0, 5% PEG-8000, 10 mM MgCl2, 10 mM DTT, 0.2 mM dNTPs, 1 mM NAD+, 4 units/mL T5 exonuclease, 25 units/mL Phusion DNA polymerase, 4,000 units/mL Taq DNA ligase) in a total reaction volume of 10-12 μL. The reactions were incubated at 50°C for 90 minutes. Gibson-assembled plasmids were used to transform *E. coli* MC1061. Gibson-assembled linear fragments were purified using spin columns, re-amplified using Phusion polymerase and used to transform PY79 or PY79 derivatives. For overlap extension PCR, 500 ng of each PCR product was mixed and standard PCR cycling was performed using end primers and Q5 polymerase (NEB). PCR fragments were routinely obtained using Phusion polymerase (NEB) or Q5 polymerase (NEB) and gel-purified before Gibson assembly or overlap extension PCR.

Individual plasmid (p) construction

pJS146: The regions 500 base pairs upstream and downstream of the *ydiOP* operon were amplified from PY79 genomic DNA using primers oJS650 and oJS651 (upstream region) and oJS653 and oJS657 (downstream region). The fragments were then combined with the pminiMAD vector using Gibson assembly.

pTN02: The *dnmA* gene was cloned from PY79 genomic DNA using primers oTN3 and oTN8 with overlapping regions to the pDR110 vector. The pDR110 vector and insert were combined using Gibson assembly.

pTN03: The *dnmA* gene was cloned from PY79 genomic DNA using primers oTN5 and oTN7 with overlapping regions to the pE-SUMO vector. The pE-SUMO vector and insert were combined using Gibson assembly.

pAS2: Overlap PCR was used to make the Y→A substitution. The 5' block was created by using oTMN5 and oAS1 with PY79 genomic DNA as a template. The 3' block was created by using oTMN7 and oAS2 with PY79 genomic DNA as a template. PCR products were gel purified and combined with the pE-SUMO vector using Gibson assembly.

pTN12: The *yabB* gene was cloned from PY79 genomic DNA using primers oTN36 and oTN37 with overlapping regions to the pE-SUMO vector. The pE-SUMO vector and insert were combined using Gibson assembly.

pTN13: The *scoC* gene was cloned from PY79 genomic DNA using primers oTN62 and oTN63 with overlapping regions to the pE-SUMO vector. The pE-SUMO vector and insert were combined using Gibson assembly.

pLVG1: To remove the *lacI* gene from pDR111_GFP(Sp) (5), the plasmid was amplified using primers oLVGLS024A and oLVGLS024B, restricted with BamHI and self-ligated with T4 DNA ligase.

pLVG1-0374: The backbone of pLVG1 without P*xyl* was amplified with primers oLVGLS023A and oLVGLS023B and combined with a DNA fragment containing U0374 (P*rsbV*), amplified from PY79 genomic DNA using primers oLVG_U0374F and oLVG_U0374R.

pLVG1-0868: The backbone of pLVG1 without P*xyl* was amplified with primers oLVGLS023A and oLVGLS023B and combined with a DNA fragment containing U0868 (P*wprA*), amplified from PY79 genomic DNA using primers oLVG_U0868F and oLVG_U0868R.

pLVG1-1292: The backbone of pLVG1 without P*xyl* was amplified with primers oLVGLS023A and oLVGLS023B and combined with a DNA fragment containing U1292 (P*yloA*), amplified from PY79 genomic DNA using primers oLVG_U1292F and oLVG_U1292R.

pLVG1-1995: The backbone of pLVG1 without P*xyl* was amplified with primers oLVGLS023A and oLVGLS023B and combined with a DNA fragment containing U1995 (P*comEA*), amplified from PY79 genomic DNA using primers oLVG_U1995F and oLVG_U1995R.

pLVG1-2292: The backbone of pLVG1 without P*xyl* was amplified with primers oLVGLS023A and oLVGLS023B and combined with a DNA fragment containing U2292 (P*ezrA*), amplified from PY79 genomic DNA using primers oLVG_U2292F and oLVG_U2292R.

Individual DNA fragment (f) construction

fLVG-1780: An upstream DNA fragment was amplified from pLVG1 using primers oLVGLS023C and oLVGLS023A. A downstream DNA was amplified from pLVG1 using primers oLVGLS023B and oLVGLS023D. A DNA fragment containing U1780(P*hbs*) was amplified from PY79 genomic DNA using primers oLVG_U1780F and oLVG_U1780R. The three fragments were assembled using Gibson assembly and the correct construct was enriched using end primers oLVGLS034 and oKJW090.

fLVG-1815: An upstream DNA fragment was amplified from pLVG1 using primers oLVGLS023C and oLVGLS023A. A downstream DNA was amplified from pLVG1 using primers oLVGLS023B and oLVGLS023D. A DNA fragment containing U1815 (P*scpA*) was amplified from PY79 genomic DNA using primers oLVG_U1815F and oLVG_U1815R. The three fragments were assembled using Gibson assembly and the correct construct was enriched using end primers oLVGLS034 and oKJW090.

fLVG-1815mut1: To replace 5'-GACGAG with 5'-GACGTG in the *scpA* promoter, an upstream and downstream DNA fragment was amplified from LVG087 genomic DNA using primer pair oLVGLS042A/oKJW89 and oLVGLS042B/oKJW090, respectively. The fragments were assembled by overlap extension PCR.

fLVG-1815mut2: To replace 5'-GACGAG with 5'-GACGCG in the *scpA* promoter, an upstream and downstream DNA fragment was amplified from LVG087 genomic DNA using primer pair oLVGLS044A/oKJW89 and oLVGLS044B/oKJW090, respectively. The fragments were assembled by overlap extension PCR.

fLVG-1815mut3: To replace 5'-GACGAC with 5'-GACGAC in the *scpA* promoter, an upstream and downstream DNA fragment was amplified from LVG087 genomic DNA using primer pair oLVGLS045A/oKJW89 and oLVGLS045B/oKJW090, respectively. The fragments were assembled by overlap extension PCR.

fLVG-2212: An upstream DNA fragment was amplified from pLVG1 using primers oLVGLS023C and oLVGLS023A. A downstream DNA was amplified from pLVG1 using primers oLVGLS023B and oLVGLS023D. A DNA fragment containing U2212 (P*rnhC*) was amplified from PY79 genomic DNA using primers oLVG_U2212F and oLVG_U2212R. The three fragments were assembled using Gibson assembly and the correct construct was enriched using end primers oLVGLS034 and oLVGLS090.

fLVG-2213: An upstream DNA fragment was amplified from pLVG1 using primers oLVGLS023C and oLVGLS023A. A downstream DNA was amplified from pLVG1 using primers oLVGLS023B and oLVGLS023D. A DNA fragment containing U2213 (P*zapA*) was amplified from PY79 genomic DNA using primers oLVG_U2213F and oLVG_U2213R. The three fragments were assembled using Gibson assembly and the correct construct was enriched using end primers oLVGLS034 and oKWJ90.

Supplementary Results

m5C modifications function as part of the BsuMI restriction-modification system.

The analysis of SMRT sequencing detected cytidine methylation in the PY79 genome **(Table 1)**. In *B. subtilis* Marburg the BsuMI RM system was first found to recognize 5' YTCGAR sites and later refined using analysis of transformation efficiency to recognize 5' CTCGAG (6). This work showed that in *B. subtilis* Marburg the *ydiO-ydiP* operon codes for the methyltransferase (MTase) responsible for m5C modifications of the BsuMI RM system and that an adjacent operon, *ydiR-ydiS-ydjA,* codes for the cognate endonuclease (6). Given the sequence similarity between the mC motif detected in the WT strain PY79, 5' CTCGARB, and the site identified in the Marburg strain, 5' CTCGAG, we decided to test whether YdiO-YdiP was responsible for cytidine methylation in PY79. Because PacBio does not robustly detect m5C methylation, we experimentally determined the modification type by treating DNA with the m5C- and 5-

hydroxymethylcytosine-specific endonuclease, MspJI **(**Supplementary **Figure S3)**. We created PY79 strains with deletions of *ydiO-ydiP* and each subunit of the putative endonuclease, *ydiR, ydiS,* or *ydjA.* DNA was purified from each of these strains in addition to WT and a strain with a deletion of N6-methyladenosine methyltransferase Δ*dnmA*, as controls. DNA from WT, Δ*dnmA*, and strains lacking *ydiO-ydiP* plus the respective restriction endonuclease subunits were treated with MspJI, recognizes 5-5hmC and m5C at 5' ^{m}CNNR sites, followed by electrophoresis on an agarose gel. Smearing in WT and Δ*dnmA* strains indicates the presence of m5C modifications whereas distinct bands in Δ*ydiOP*Δ*ydiR,* Δ*ydiOP*Δ*ydiS,* Δ*ydiOP*Δ*ydjA* strains indicates loss of m5C modifications, implicating *ydiOP* as the MTase responsible for all m5C methylation in the *B. subtilis* genome (Supplementary **Figure S3**). The results we present here confirm the BsuMI RM recognition site as 5'CTCGARB in *B. subtilis* strain PY79. The m5C motif identified in PY79 was not detected as modified in NCIB 3610 by PacBio SMRT sequencing **(Table 1)**.

***B. subtilis* m6A does not function in replication timing.** We sought to determine the consequence of m6A loss in *B. subtilis* cells. In the Gram-negative bacterium *E. coli*, GATC-specific m6A functions in origin sequestration (7-9), DNA mismatch repair (10,11), and the regulation of gene expression (12). The methylation status of palindromic GATC sites in the *E. coli* origin of replication regulates the binding of SeqA, which inhibits origin firing by sequestering the origin region (7-9). Whereas GATC sites are enriched in the *E. coli* origin, as discussed in the main text the m6A motif is not present in the *B. subtilis* replication origin, although a high density of m6A sites flank the origin on the left arm **(Fig 1)**. To empirically determine if m6A sites located in the origin proximal region on the left arm influence origin duplication, we assessed the origin proximal copy number in exponentially growing WT and Δ*dnmA* (M.BsuPY79I) cells

using Spo0J-GFP (*parB-gfp*) as a marker for origin copy number as done previously (13,14). We show that in WT, Δ*dnmA,* Δ*yabB* cells, 65%, 64%, 66% of cells showed two Spo0J-GFP foci, respectively. As controls we used a deletion of *yabA*, a negative regulator of origin firing (15), and show that 74% of cells have four or more foci as expected (14). As a hypo-initiation control we used an IPTG regulated promoter (P_{spac}*dnaAN*) to deplete the replication initiation protein *dnaA* and the replication sliding clamp *dnaN*. We show a near 8-fold increase in the percentage of cells with a single Spo0J-GFP focus, demonstrating an inhibition of DNA replication initiation (14) **(**Supplementary **Figure S4)**. With these results we show no difference in origin proximal copy number between WT, Δ*dnmA,* or Δ*yabB* cells as determined by fluorescence microscopy and we conclude that m6A does not contribute to the regulation of DNA replication initiation.

B. subtilis **m6A does not function in DNA mismatch repair.** In addition to origin sequestration, methylation at GATC sites in *E. coli* also functions in strand discrimination during DNA mismatch repair, thereby ensuring removal of mismatched bases from the nascent strand (10). Both the loss of adenosine methylation at GATC sites and hyper-methylation of the chromosome by overexpression of Dam resulted in an increase in spontaneous mutation rate (16,17). m6A sites are non-palindromic in *B. subtilis* and occur far less frequently (~1,200 sites relative to ~20,000 GATC sites in *E. coli*). The lack of an even distribution on the leading and lagging strands across the genome and the low number of sites does not support a contribution of m6A to strand discrimination during mismatch repair. To be certain, we conducted rifampin resistance assays as a measure for mutation rate (1,18,19) in WT and Δ*dnmA* strains. No difference in mutation rate between these strains was observed as compared to a mismatch repair deleted control **(**Supplementary **Table S5)**. These results indicated that the presence or absence

of m6A does not influence spontaneous mutagenesis in *B. subtilis* (20,21). Furthermore, because the m6A sites occur multiple times at the *addA* locus and AddA is important for recombinational repair (22), we performed spot titer assays to determine if Δ*dnmA* cells were more sensitized to DNA damaging agents relative to WT cells and found no increase in sensitivity **(**Supplementary **Figure S8)**.

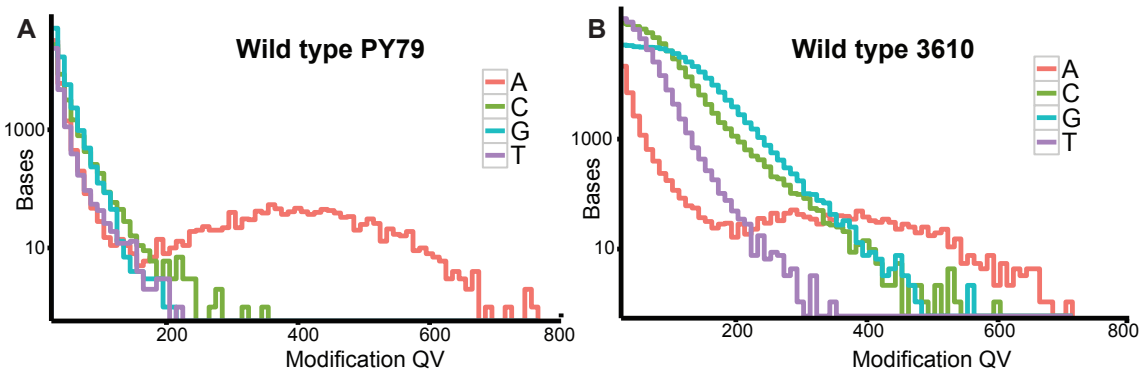

Supplementary Figure S1. The genome of *B. subtilis* strains contain m6A modifications. (A) PacBio SMRT sequencing of genomic DNA isolated from WT PY79 cells. Modification quality values (modQVs) indicate if the kinetics of the DNA polymerase differs from the expected background at a particular locus, where a modQV of 30 represents a p-value of 0.001. ModQVs are indicated on the x-axis and the number of bases is indicated on the y-axis. Each line represents the modification quality values for a particular nucleotide. **(B)** PacBio SMRT sequencing of genomic DNA isolated from the WT ancestral strain NCIB 3610.

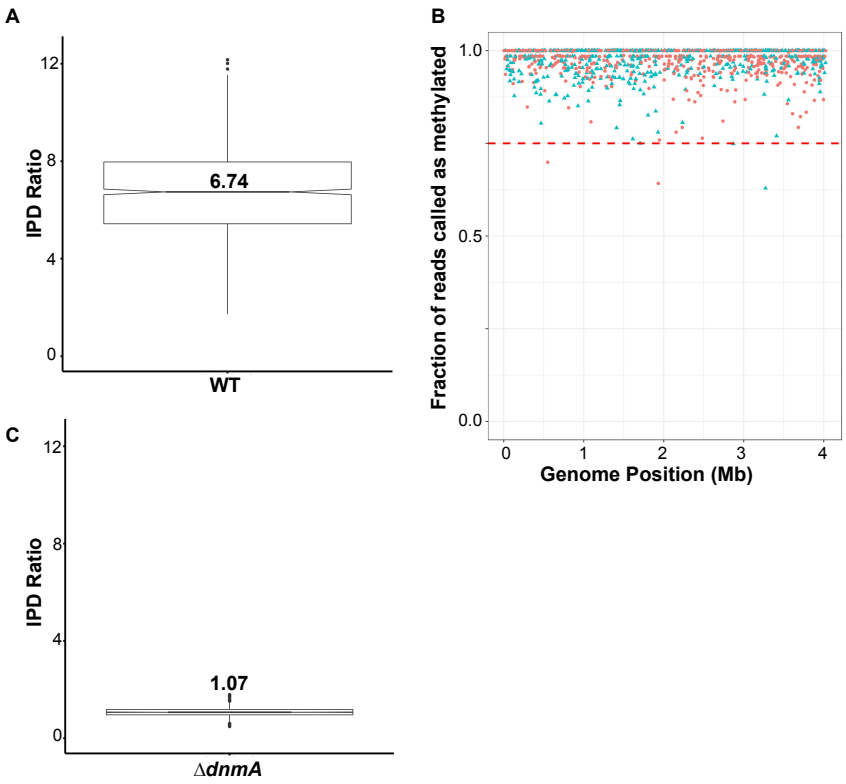

Supplementary Figure S2. GACG^{m}AG sites have high modification scores throughout the *B. subtilis* PY79 genome. (A) Representative boxplot of interpulse duration (IPD) ratio values at GACGAG sites throughout the genome in WT cells. The median IPD ratio value is indicated. **(B)** The genomic location of each GACG^{m}AG site (x-axis) and the corresponding fraction of reads that were called as methylated at that position (y-axis) from PacBio SMRT sequencing is plotted. Sites that appear on the plus strand are indicated as a green triangle and those that appear on the minus strand are indicated as red dots. **(C)** Representative boxplot of the IPD ratio values at GACGAG sites throughout the genome in Δ*dnmA* (M.BsuPY79I) cells. Median IPD ratio value is indicated.

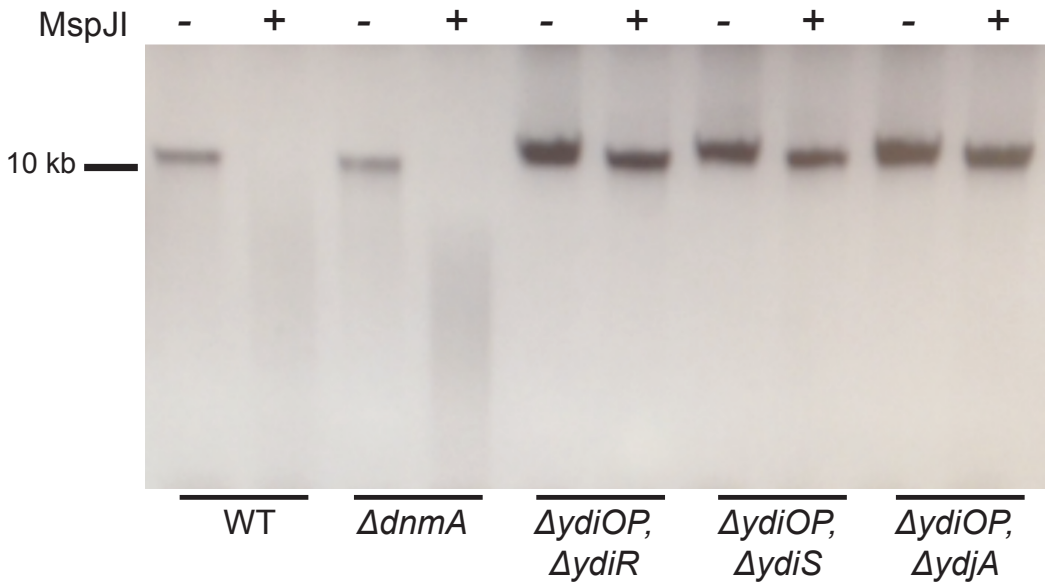

Supplementary Figure S3. Deletion of the BsuMI RM system eliminates m5C from the *B. subtilis* chromosome. Clean deletions were made for the coding regions of both subunits of the putative methyltransferase (*ydiOP*) in conjunction with separate deletions for each gene in a nearby operon coding for a putative restriction endonuclease (*ydiR, ydiS, ydjA*). DNA purified from these strains was subjected to 6 hours of treatment with a 5-methylcytidine and 5-hydroxymethylcytidine specific endonuclease MspJI. (-) indicates no treatment, (+) indicates treatment with MspJI.

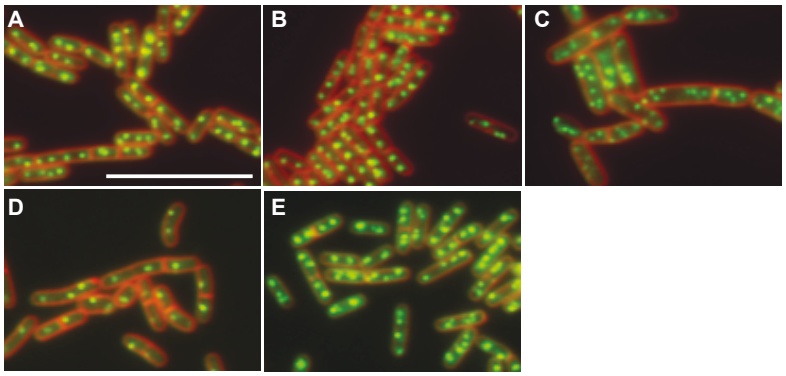

F

Relevant genotype	No. of cells	Percentage of cells with *n* Spo0J-GFP foci				
		1	2	3	4	>4
wild type	1079	6	65	15	14	<1
Δ*dnmA*	1083	7	64	13	15	1
yabA::cat	1059	3	8	9	12	74
DnaAN depletion	1072	47	40	7	3	5
Δ*yabB*	1029	2	66	15	15	2

Supplementary Figure S4. Origin firing in *B. subtilis* is not regulated m6A. (A-E) Representative images of fluorescence microscopy for (A) WT, (B) Δ*dnmA*, (C) *yabA::cat*, (D) *dnaAN* depletion, and (E) Δ*yabB* strains expressing *spo0J::spo0J-gfp*, respectively. White bar = 10 μm. **(F)** Quantification of Spo0J-GFP foci for strains A-E.

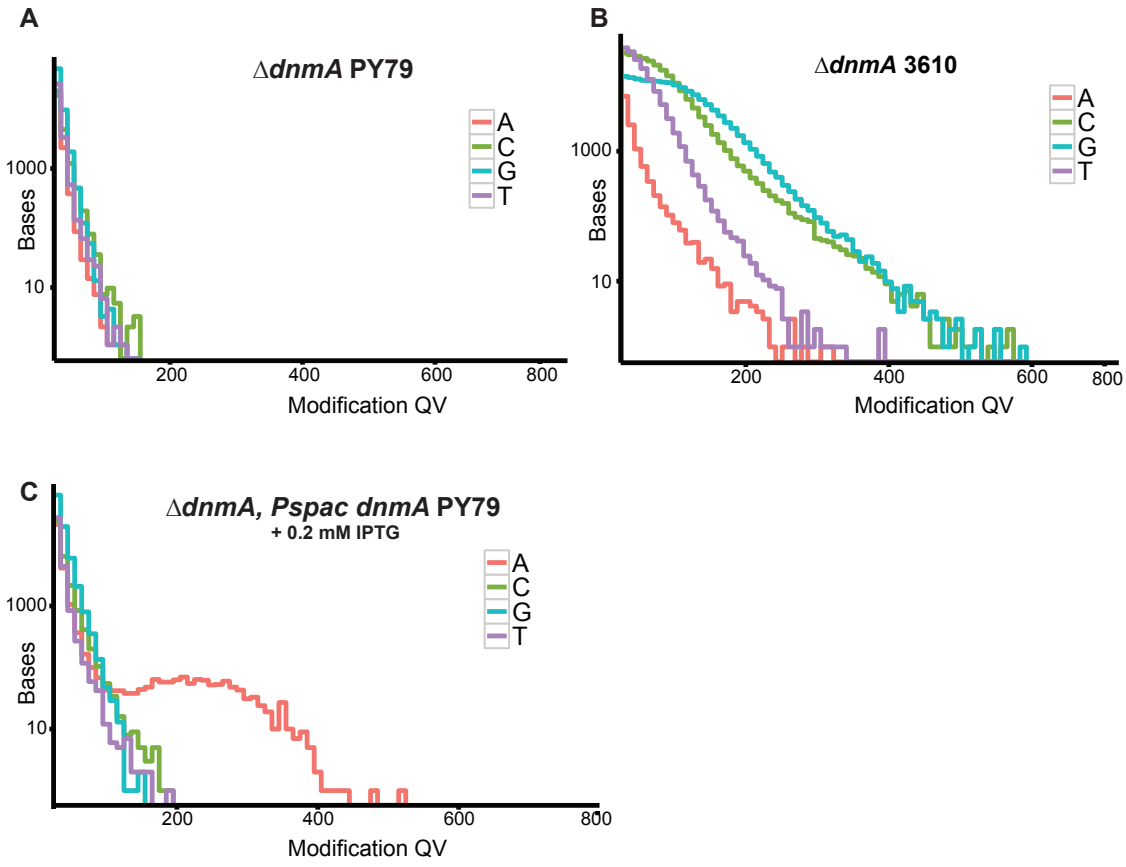

Supplementary Figure S5. *Bacillus subtilis* m6A modifications are dependent on methyltransferase DnmA. (A) PacBio SMRT sequencing of genomic DNA isolated from the Δ*dnmA* PY79 strain. **(B)** PacBio SMRT sequencing of genomic DNA isolated from the ancestral strain NCIB 3610 with a *dnmA* deletion. **(C)** PacBio SMRT sequencing of genomic DNA isolated from Δ*dnmA* cells ectopically expressing *dnmA* from the *amyE* locus with 0.2 mM IPTG.

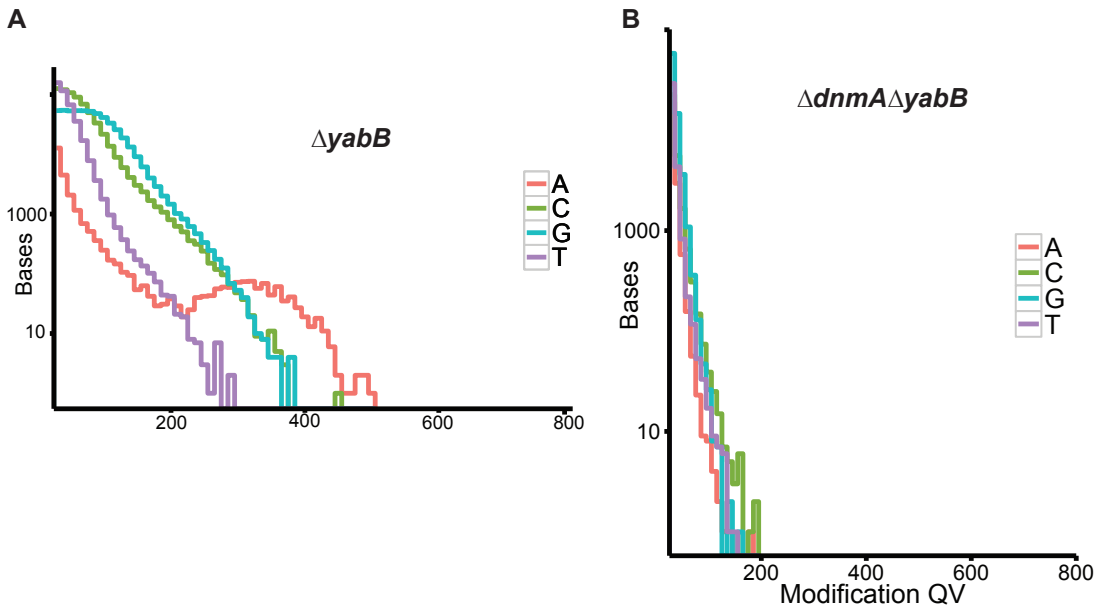

Supplementary Figure S6. Genomic m6A is present in a *yabB* deletion strain. (A) PacBio SMRT sequencing of genomic DNA isolated fromPY79 Δ*yabB* cells. **(B)** PacBio SMRT sequencing of genomic DNA isolated from PY79 Δ*dnmA*Δ*yabB* cells.

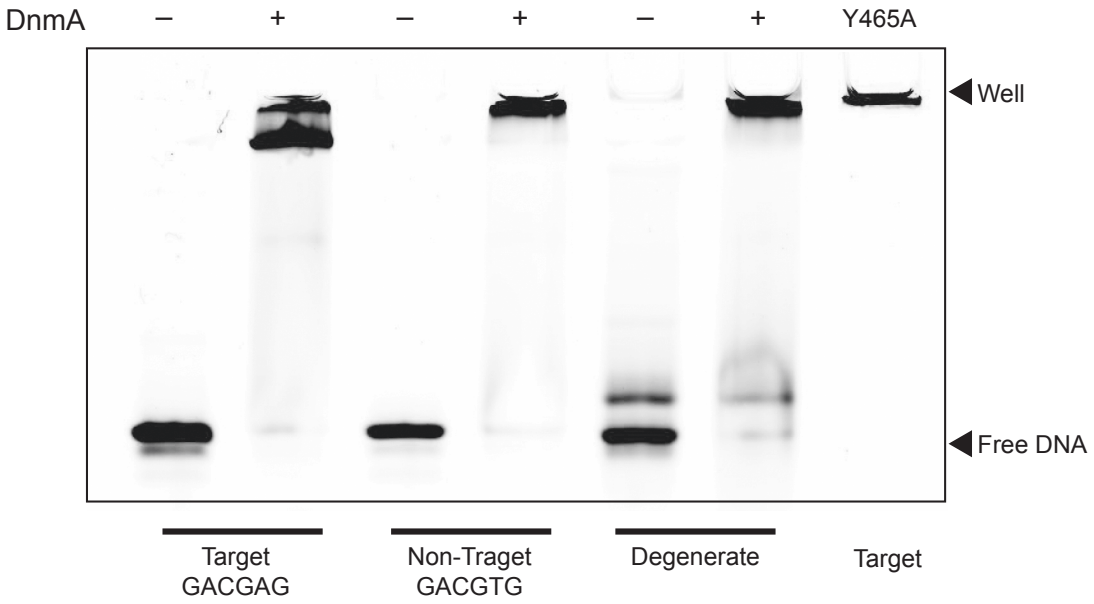

Supplementary Figure S7. DnmA binds DNA without the m6A motif. DnmA (M.BsuPY79I) substrate binding was determined by electrophoretic mobility shift assay (EMSA) with purified DnmA and varying substrates. 5' IR-labeled substrates include: target substrate (GACGAG), non-target substrate (GACG**T**G) and a degenerate sequence substrate, which are indicated at the bottom. The (-) indicates the absence of DnmA from the reaction, (+) indicates addition of DnmA to the reaction. As indicated, the final lane includes the DnmA catalytic inactive variant (Y465A) incubated with the target substrate.

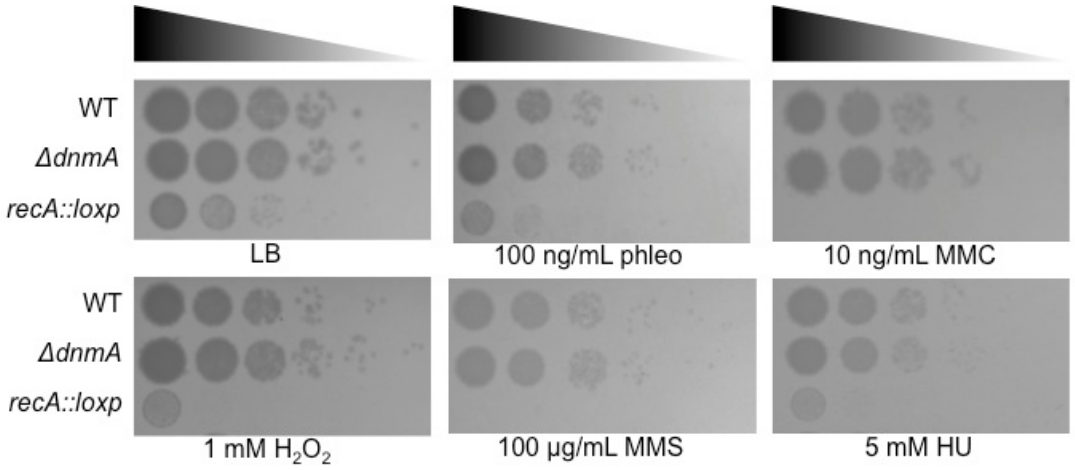

Supplementary Figure S8. Loss of m6A does not cause an increased susceptibility to genotoxic stress. WT and Δ*dnmA* cells were tested for their sensitivity to several DNA damaging agents and replication fork stress caused by hydroxyurea (HU). Cells were grown to mid-exponential growth phase, serially diluted, and plated on LB agar plates with the following concentrations of DNA damaging agents: 100 ng/mL phleomycin (phleo), 10 ng/mL mitomycin C (MMC), 1 mM hydrogen peroxide (H_2O_2), 100 µg/mL methyl methanesulfonate (MMS), and 5 mM hydroxyurea (HU). Cells with a *recA::loxP* disruption were used as a control.

Supplementary Table S1. Strains used in this study

Strain	Genotype	Source
JWS10	PY79	(23)
JWS261	Δ*ydiOP,* Δ*ydiR*	This work
JWS262	Δ*ydiOP,* Δ*ydiS*	This work
JWS263	Δ*ydiOP,* Δ*ydjA*	This work
TMN1	Δ*yabB*	This work
TMN5	Δ*dnmA* (*M.BsuPY79I*)	This work
TMN7	Δ*dnmA,* Δ*yabB*	This work
DK1042	NCIB 3610 *comIQ12I*	(24)
TMN47	NCIB 3610*,* Δ*dnmA* (*M.Bsu3610I*)	This work
TMN16	Δ*dnmA, amyE::*P_{spac}*dnmA*	This work
JWS259	*spo0J::spo0J-gfp*	
JWS260	Δ*dnmA, spo0J::spo0J-gfp*	This work
TMN80	Δ*yabB, spo0J::spo0J-gfp*	This work
AK42	*yabA::cat, spo0J::spo0J-gfp*	Lab stock
LAS254	P_{spac}*dnaAN::cat, spo0J::spo0J-gfp*	(14)
BTS13	Δ*mutSL::spc*	(25)
LVG066	*amyE::PrbsV-GFP*	This work
LVG067	Δ*dnmA, amyE::PrbsV-GFP*	This work
LVG068	*amyE::PwprA-GFP*	This work
LVG069	Δ*dnmA, amyE::PwprA-GFP*	This work
LVG070	*amyE::PyloA-GFP*	This work
LVG071	Δ*dnmA, amyE::PyloA-GFP*	This work
LVG072	*amyE::PzapA-GFP*	This work
LVG073	Δ*dnmA, amyE::PzapA-GFP*	This work
LVG074	*amyE::PrnhC-GFP*	This work
LVG075	Δ*dnmA, amyE::PrnhC-GFP*	This work
LVG079	*amyE::PcomEA-GFP*	This work
LVG080	Δ*dnmA, amyE::PcomEA-GFP*	This work
LVG081	*amyE::PezrA-GFP*	This work
LVG082	Δ*dnmA, amyE::PezrA-GFP*	This work
LVG087	*amyE::PscpA-GFP*	This work
LVG088	Δ*dnmA, amyE::PscpA-GFP*	This work
LVG102	*amyE::PscpA mut1-GFP*	This work
LVG103	Δ*dnmA, amyE::PscpA mut1-GFP*	This work
LVG105	*amyE::Phbs-GFP*	This work
LVG106	Δ*dnmA, amyE::Phbs-GFP*	This work
LVG108	Δ*dnmA operon, amyE::PscpA-GFP*	This work
LVG109	Δ*dnmA operon, amyE::PscpAmut1-GFP*	This work
LVG118	*amyE::PscpA mut2-GFP*	This work
LVG119	Δ*dnmA operon, amyE::PscpAmut2-GFP*	This work

LVG120	*amyE::PscpA mut3-GFP*	This work
LVG121	Δ*dnmA operon, amyE::PscpAmut3-GFP*	This work

Supplementary Table S2. Plasmids used in this study

Plasmid	Vector	Insert	Source
pJS146	pminiMAD	*ydiOP*	
pTN02	pE-SUMO	*dnmA* (*M.BsuPY79I*)	
pTN03	pDR110	*dnmA* (*M.BsuPY79I*)	
pAS2	pE-SUMO	*dnmA (Y465A)* (*M.BsuPY79I*)	
pTN12	pE-SUMO	*yabB*	
pTN13	pE-SUMO	*scoC*	
pLVG1	pDR111_GFP(Sp)	w/o lacI	(5)
pLVG1-0374	pLVG1	P*rsbV*/U0374	
pLVG1-0868	pLVG1	P*wprA*/U0868	
pLVG1-1292	pLVG1	P*yloA*/U1292	
pLVG1-1995	pLVG1	P*comE*/U1995	
pLVG1-2292	pLVG1	P*ezrA*/U2292	
pHP13		None	BGSC (http://www.bgsc.org)

Supplementary Table S3. Oligonucleotides used in this study

Oligo name	Oligo sequence
oAS1	CCAAGAGCCGGTGGATTACCAAAAACATATACTTCTTC
oAS2	CCACCGGCTCTTGGTTCAAAAAAACAAAACAAAGAACATAAATC
oAS9	/5IRD700/GTGCAGCGTATCCGGACAATGACGAGACGGAAACAGAGCTGCTGCTG ATC
oAS10	/5IRD700/GTGCAGCGTATCCGGACAATGACGTGACGGAAACAGAGCTGCTGCTGATC
oAS11	/5IRD700/ATATAAACATACATACATACATTATTATATAAACATACATACATACATTA
oTMN5	GGCTCACCGCGAACAGATTGGAGGTATGGCGCTCATTGATTTAGAAGA TAAAATTGC
oTMN7	TGGTGGTGGTGGTGGTGCTCGACTACCGTTCTGTCATTTCTTGATACAA TTTAAGCAATAC
oTMN36	CACCGCGAACAGATTGGAGGTATGGTTTCATTACATGATGATGAAAGATTAGATTA
oTMN37	TGGTGGTGGTGGTGCTCGATTATTTGTCTCCATATAAAATGGTCCTGATTTC
oTMN38	GTGCAGCGTATCCGGACAATGACGAGACGGAAACAGAGCTGCTGCTGATC
oTMN39	GATCAGCAGCAGCTCTGTTTCCGTCTCGTCATTGTCCGGATACGCTGCAC
oTMN40	GTGCAGCGTATCCGGACAATGACGTGACGGAAACAGAGCTGCTGCTGATC
oTMN41	GATCAGCAGCAGCTCTGTTTCCGTCACGTCATTGTCCGGATACGCTGCAC
oTMN62	CACCGCGAACAGATTGGAGGTATGAATCGAGTGGAACCGCCCTATG
oTMN63	GGTGGTGGTGGTGGTGCTCGATTAACTGTTTACAGGTTCGAGCTCTTCAG
oTMN67	/5IRD700/CA AAACAGGATATGAAATAGTATTGGACGAGAGCTTTTTGGTGGCTTATACTATAG
oTMN68	/5IRD800/CTATAGTATAAGCCACCAAAAAGCTCTCGTCCAATACTATTTCATATCCTGTTTTG
oTMN70	/5IRD700/CAAAACAGGATATGAAATAGTATTGGACGTGAGCTTTTTGGTGGCTTATACTATAG
oTMN71	/5IRD800/CTATAGTATAAGCCACCAAAAAGCTCACGTCCAATACTATTTCATATCCTGTTTTG
oJR269	TAATGTATGTATGTATGTTTATATAATAATGTATGTATGTATGTTTATAT
oJR270	GUGCAGCGUAUCCGGACAAUGACGAGACGGAAACAGAGCUGCUGCUGAUC
oJR271	GAUCAGCAGCAGCUCUGUUUCCGUCUCGUCAUUGUCCGGAUACGCUGCAC
oLVGLS023A	GCTAGCTGATTAACTAATAAGGAGGACAAAC
oLVGLS023B	GAGAGTCGAATTCCTGCAGC
oLVGLS024A	CCGGGATCCGATGACCTCGTTTCCACCGAATTAGC
oLVGLS024B	CCGGGATCCGCAGGCCATGTCTGCCCGTATTTC
oLVGLS034	CGTATCACGAGGCCCTTTCG
oLVGLS042A	GAAATAGTATTGGACGTGAGCTTTTTGGTGGCTTATAC
oLVGLS042B	GCCACCAAAAAGCTCACGTCCAATACTATTTCATATCCTG
oLVGLS044A	GAAATAGTATTGGACGCGAGCTTTTTGGTGGCTTATAC
oLVGLS044B	GCCACCAAAAAGCTCGCGTCCAATACTATTTCATATCCTG
oLVGLS045A	GAAATAGTATTGGACGACAGCTTTTTGGTGGCTTATAC
oLVGLS045B	GCCACCAAAAAGCTGTCGTCCAATACTATTTCATATCCTG
oKWJ89	TTCTTCGCTTGGCTGAAAAT
oKWJ90	CACCAGGTTTTTGGTTTGCT
oLVG52A	5'Biotin-CTGCAGGAATTCGACTCT
oLVG52B	5'-Biotin-CCTTATTAGTTAATCAGCTAGC
oLVG_U0374F	CGCCATTCGCCAGGGCTGCAGGAATTCGACTCTCCCTGATCTGCAGAAGCTCATTG
oLVG_U0374R	CATGTTTGTCCTCCTTATTAGTTAATCAGCTAGCCTTCAAATCACTAGTTGCTTTATAC

oLVG_U0868F	CGCCATTCGCCAGGGCTGCAGGAATTCGACTCTCGGTCTGCATTTGCCAATTG
oLVG_U0868R	CATGTTTGTCCTCCTTATTAGTTAATCAGCTAGCAAAATAATGAATCTCCTTGAAGG
oLVG_U1292F	CGCCATTCGCCAGGGCTGCAGGAATTCGACTCTCGTTAATCCTTGTTTCATGGACG
oLVG_U1292R	CATGTTTGTCCTCCTTATTAGTTAATCAGCTAGCTCTCATTCTTCCTGCATTCGAT
oLVG_U1995F	CGCCATTCGCCAGGGCTGCAGGAATTCGACTCTCGCGTGACAGCTGATTTTACGG
oLVG_U1995R	CATGTTTGTCCTCCTTATTAGTTAATCAGCTAGCCGCAGTGAAAAAGCAGTTTC
oLVG_U2292F	CGCCATTCGCCAGGGCTGCAGGAATTCGACTCTCCGGAAGTATTGAAGTCGAG
oLVG_U2292R	CATGTTTGTCCTCCTTATTAGTTAATCAGCTAGCCGGAGTATCTATTCTTCCATTG
oLVG_U1780F	CGCCATTCGCCAGGGCTGCAGGAATTCGACTCTCGAATCATAAACGAAGGCTCTGG
oLVG_U1780R	CATGTTTGTCCTCCTTATTAGTTAATCAGCTAGCGTAGAGTAACACATATAAAAAGCCAT
oLVG_U1815F	CGCCATTCGCCAGGGCTGCAGGAATTCGACTCTCCTCTAGTGCTTCTTAGAAAGG
oLVG_U1815R	CATGTTTGTCCTCCTTATTAGTTAATCAGCTAGCTCACTCTCATTGCCGGAAAAAC
oLVG_U2212F	CGCCATTCGCCAGGGCTGCAGGAATTCGACTCTCGTAAGTGAACCGCTGTACG
oLVG_U2212R	CATGTTTGTCCTCCTTATTAGTTAATCAGCTAGCATTCCGCGAGAATCCTAG
oLVG_U2213F	CGCCATTCGCCAGGGCTGCAGGAATTCGACTCTCGTGAAGTGCTGGCCGTAAATG
oLVG_U2213R	CATGTTTGTCCTCCTTATTAGTTAATCAGCTAGCACTTTTCGCTGTATATACCAGTG

Oligo sequences in red represent RNA. /5IRD700/ indicates 5' infrared dye label with excitation at 700 nm.

Supplementary Table S4. Modified motifs detected in *B. subtilis* by PacBio SMRT sequencing.

Motif	Type	%Detected	Mean QV	Mean Cov.	Mean IPD Ratio
WT PY79					
GACG**A**G	m6A	99.7	388	286	6.72
V**T**TCGAGNR	NA	79.2	75	284	1.90
CTCGARB	m5C*	70.8	74	270	1.89
V**T**TVGAGNBY	NA	40.1	55	283	1.67
GGNB	NA	5.6	41	290	1.67
WT 3610					
GACG**A**G	m6A	94.7	362	313	4.84
R**A**WKYAGYA	m6A	28.7	98	309	1.66
D**T**NRADDDG	NA	22.8	61	305	1.78
D**T**WTWGAAG	NA	21.4	57	327	1.71
AGCNMAAAWH	m6A	15.8	107	322	1.53
TNNNDNNH	NA	12.6	61	303	1.78
D**T**SNVCNTWNH	NA	11.7	58	304	1.75
TWGCNNNG	NA	10.6	58	313	1.75
TNRGCYNH	NA	10.1	56	309	1.72
TNNNCRVH	NA	9.6	58	304	1.76
TSNNNNNG	NA	6.1	57	305	1.75
AGDNNNNW	m6A	4.3	104	325	1.71

*Modification type confirmed via methylation sensitive restriction endonuclease digest.
The motifs shown in this table are comprehensive to those presented in Table 1 in the main text.

Supplementary Table S5. Cells with Δ*dnmA* are wild type for mutation rate

Strain	No. of cultures	Mutations per culture	Mutation rate (Mutations per generation 10^{-8} ± [95%CI]	Relative mutation rate
Wild Type	20	0.60	1.7 [0.95-1.68]	1
Δ*dnmA*	22	0.72	1.8 [0.94-2.2]	1.05
Δ*mutSL*	22	41.3	120.8 [109-131]	71.1

Mutagenesis assays were done as described using rif^R as an indicator. Mutation rate and mutations per culture were calculated using the Ma-Sandri-Sarkar Maximum Likelihood Estimator with the web-based tool FALCOR (2). Data and calculations supporting this table are publicly available https://figshare.com/articles/Nye_et_al_DnmA_methyltransferase/8070995.

Supplementary Table S6. Modified motifs detected in *B. subtilis* by PacBio SMRT sequencing.

Motif	Type	%Detected	Mean QV	Mean Cov.	Mean IPD Ratio
***ΔdnmA* WT PY79**					
V**T**TCGAGNR	NA	62.5	53	118	2.00
CTCGARB	m5C*	46.7	51	120	2.00
***ΔdnmA* WT 3610**					
V**A**TATRGCA	m6A	54.0	88	363	2.00
R**A**HKYAGYA	m6A	31.0	110	357	1.67
DD**T**NRGCNTHNH	NA	20.4	60	356	1.72
DNND**T**GYAADNG	NA	20.3	65	348	1.81
D**T**NRVDDDG	NA	15.2	61	355	1.73
TNNNDNNH	NA	12.3	62	353	1.74
TNNNCRVH	NA	9.4	60	359	1.72
AGNNMRNA	m6A	9.1	109	359	1.55
TNNSCBDH	NA	7.2	58	363	1.68
TSNNBNNG	NA	6.4	58	361	1.71
AGNNDNNW	m6A	3.4	101	365	1.54
ANDNNNNH	m6A	0.8	98	367	1.53
***ΔdnmA, amyE::Pspac dnmA* PY79**					
GACG**A**G	m6A	99.7	213	152	6.32
V**T**TCGAGNR	NA	67.2	59	146	1.98
CTCGARB	m5C	52.7	59	149	2.00
MNGACG**A**WCC	NA	47.3	58	152	2.20
V**T**TCGAGBB	NA	38.1	53	157	1.82
WAGACG**A**WB	NA	21.7	53	148	2.19
GGNNB	NA	6.6	40	168	1.86

*Modification type confirmed via methylation sensitive restriction endonuclease treatment.
The motifs shown in this table are comprehensive to those presented in Table 2 in the main text.

Supplementary Table S7. PacBio SMRT sequencing at GACGAG motifs in WT PY79.
Please see attached excel file providing information on all GACGAG motifs in PY79.

Supplementary Table S8. PacBio SMRT sequencing at GACGAG motifs in Δ*dnmA* in PY79. Please see attached excel file providing information on all GACGAG motifs in PY79 Δ*dnmA*.

Supplementary Table S9. Modified motifs detected in *B. subtilis* by PacBio SMRT sequencing.

Motif	Type	%Detected	Mean QV	Mean Cov.	Mean IPD Ratio
ΔyabB					
GACG**A**G	m6A	96.9	304	240	5.15
ATATRGCA	m6A	74.0	80	238	2.09
ADGYACYTV	m6A	34.7	85	238	2.01
ADKYASYA	m6A	29.8	88	238	1.88
AGCNAAAAWH	m6A	17.3	95	237	1.58
G**A**NNBNRCA	m6A	13.7	98	241	1.90
TNNNNNNH	NA	12.2	46	234	1.69
D**T**VVVNNDG	NA	11.1	44	234	1.67
ANVBANYW	m6A	6.4	78	238	1.81
AGDNVDNW	m6A	5.4	87	236	1.81
TBNNDNNG	NA	5.2	43	235	1.67
AGBB	m6A	2.7	99	238	2.02
ΔdnmA ΔyabB					
V**T**TCGAGNR	NA	71.9	60	166	1.92
CTCGARB	NA	57.3	57	168	1.91
V**T**TCGAGBY	NA	33.2	46	181	1.70
GG	NA	3.1	39	185	1.77

Supplementary Table S10. Identification of protein species in DnmA protein purification

Identified Protein Accession Number	Molecular Weight	Total Spectrum Count
YEEA_BACSU	101 kDa	190
SMT3_YEAST	12 kDa	42
K2C1_HUMAN	66 kDa	34
HORN_HUMAN	282 kDa	34
TRYP_PIG	24 kDa	18
K1C10_HUMAN	59 kDa	19
K22E_HUMAN	65 kDa	21
K1C9_HUMAN	62 kDa	15
K2C5_HUMAN	62 kDa	4
CYTA_HUMAN	11 kDa	3
K1C14_HUMAN	52 kDa	8
ALBU_HUMAN	69 kDa	2
ARGI1_HUMAN	35 kDa	3
ANXA2_BOVIN (+8)	39 kDa	2
FABP5_HUMAN	15 kDa	2
SBSN_HUMAN	61 kDa	2

Mass spectrometry was completed by the University of Michigan Core on the high molecular weight species, confirming the presence of DnmA (YeeA). The SMT3_Yeast contaminant is likely the result of trace SUMO-tagged DnmA from the protein purification process (see Materials and Methods).

Supplementary Table S11. Promoter upshifts containing the m6A motif

Upshift	Sequence context	Downstream TU
U374	cgatgattttacgttaattgttttgcggagaaaGGTTTAAcgtctgtgtcagacgaGGGTATAAAGCAACTAGTGatttgaaggaaaatttgaggtgatacga	**rsbV, rsbW, sigB, rsbX**
U868	atattccaaatcatttaaaataaccttaaaattcccctgtaagcggtatctcgtcctatgaaatTATGATACCTTCAAGGAGATtcattattttgcaggagg	**wprA**
U1292	gctctcttatagagatatcactctataagcatgcttaTTCTGActcgtccccatttCATGCTATAATTATCGAATGcaggaagaatgagagggtgtattgca	**yloA**
U1780	aaaaaaggaatattcgttcggtaaatcaccttaaatcCTTGACgagcaagggattgacgCTTTAAAATGCTTGATATGGctttttatatgtgttactctac	**S861, hbs**
U1815	ctgtacaaactccttcaaaacaggatatgaaatagTATTGGACgagagcttttggTGGCTTATACTATAGGGTAGccagtttttccggcaatgagagtga	**scpA, spcB, ypuI**
U1995	taaaacgatggttttttaaaatgctttttatgCTTTTGCAgtacagacgaacgTATGACATACTCGTCTACACatgaaactgcttttcactgcggaaat	**S963, comEA-EC, S962, holA**
U2212	tgtatataccagtgtatcataacagcgggaggctcgtcTTTCCATTcatttaataaaCGTGTTATGATAAGAACTAGgattctcgcggaatggaggagaaa	**yshA (zapA), yshB, S1080, polX, mutSB**
U2213	gttcttatcataacacgtttattaaatgaatggaaagacgagcctcccgctgtTATGATACACTGGTATATACagcgaaaagtgtaaaaaaaggagattat	**rnhC**
U2292	aatttttggacgagtgtgatgtgaccgactctttTGGCTTATaaacgccgagaGATGCTACAATGGAAGAATAgatactccggtaatattgttcatatac	**S1127, S1125, ezrA**
U2511	acggatgggcacgttagatccttacgatttttctgctgacTCGTCAATttgaacggcaaTATGGTATAATTAATAACAAttttcatttaggaggcaattt	**yumC**
U624	cactaaagttgatcaaatgacctaagtgcgccaaacgtGTTACGggacgagctatctCATGGTATAAAATGGAATTGTaaacgttatcaaggaggtcgtcat	**malA, malR-Q**
U792	atattcagctcagtccttttgatgcgtctttcccgCACATAActcgtctcattcccGCATATGGTTAAGAATAAAgaatctatgcaaaggggggaggagcc	**yhaL**
U1042	agcggtctgaggctttttattagataaaagacctaattgttctaTGAAACTTTCtgacgagatatCCGTATATCATACAGAttgacatcattcacatcaga	**S462, S461**
U1293	tacaccctctcattcttcctgcattcgataattatAGCATGaaatggacgagtcaGAATAAGCATGCTTATAGAgtgatatctctataagagagcagggg	**yloB, S571, yloC, ylzA, gmk, rpoZ**
U1406	atgtgttcataaaaaactaaaaaaaaTATTGAAAatactgacgaggttATATAAGATGAAAATAAGTTagtttgtttaaacaacaaactaataggtgatgt	**S634, xylA, S635, xylB, S636**
U1861	ctttcccgtcatataaactgctcaaatgaaccgcttttgtcaaacaTTTCTGTATAATAGACGAGAaatcagtttatttttcagtatagaagcatttttat	**yqjN**
U2116	atcaagggaataaagatcgttttatgacgagccaaaagggtgaccatAACATAtcaagcataaaaaagACATAGACTGTTAACAGAAccagcaaacaaat	**S1041, glnQ, glnH, glnM, glnP**
U2235	gtgtattggctttgcggaaaaaagggtggaacCacgattccgttattcaaCCTCGTCCCTttcataggggcggggtttttatatgcaaaaaaaggagtg	**thrS**
U2676	cttactttaaaaagccacgcaacacggttctCGtcacagacgaagaggccgcAaagaagttattaagggatgaataatccctcaatataaatatctctcac	**gapA, S1301, S1300, pgk, tpiA, pgm, eno**
U3059	gcgaaacacacatgttctccactaaaaaagAGTATAtccggtatagatagaCGAGAAACTGAAAGGGAAAcctcattcgtttacatattggcttcagcgga	**aldY**
U75	cctgatttccaaatcatttgcggatcgcctgaacTGCttgtcagcaaaaagggcAAGCTATTAGAGACGAGACcgattgcgggcacccgttccagagggaa	**secondary internal pabB upshift**
U568	aaaagagtatctcgtatagaacataagaagaatgacgagtttttaAGATTAtcatcaattatgtgaGAATAAAATATTATAAGGGaaaatgaaggctgtc	**S257 - as-fecF**
U797	ctatttttctttttttgcagatgattgGCAGGACATggatgactttaTGTACAAATAAAATAACGAcgagcaaaccgccgaataaagatacatattcatcg	**as-yhaJ; secondary yhaI upshift**
U809	tttgctgcggaagacatatacagataaagaacagccATAATGacatagacgagaagcGCATACATATAAACAGATTggaaaacaaaataaagaacgagtgt	**as-ecsB (ecsB internal)**
U895	aagaaggtccgtattaatttttcccaCTCATAAaccttacttttacccCACCATACTATTgaagacgactcatctcgtcaaagtatggaaggggcagtctc	**S397, yizC**
U911	tcctgagaaggttttaacaaatcatgatcttgaaaaaatggtTGAAACTTCTgacgagtggatTCGTACAAGAACAGGAatagaagaaagaagaatcgcag	**secondary internal fabHA upshift**
U936	ataaaacattctaaaggcggtgtttccgacggcttcggctcgtcgccaAGCATCtcaaataaaatttctTCATATACATCATATGAGTagctgccaggaac	**S416 - as-spxH**
U1010	cgggtagccgaccttcggattatcaAACTTGACgagcagcggcatcACGGCCACACTTGTGATAAAcaaggcgccaagtgatccgatttggcggaacgtcg	**as-yjmB**
U1122	gttcttaacggttatatgaaccaattcattcgaaaagacaCCTTTACAaacatacgttcgttaAATTATAATAAAACAGACGAgctgccatccagcatccc	**S498; independent transcript**
U1389	ttgttgttgatattcttgaataaaaaaacccggtttctCGCGAtgaggagccgggttttttatGAGACGCTCGTCCCCGTCtcggctatgattctaggat	**S623 - as-cwlC**
U1429	gaatgtaggtctctttgaggctttagcacgaattctctcgtcctccttgttaaatttttgttaaattcaCAATATTATAtaccattagcccgggcgctgtt	**S653 - secondary internal surA upshift**
U1984	aaatattttattcaaagtcagccagtcgacgagTATTTAAacgcactcgaacaGGAAATGATAAAtacaatagcaaaaaccgggcagcctgatctcaaaac	**secondary hrcA-grpE-dnaK upshift**
U2466	tcatttcttttggcgttacgtcattcatcctcgtcatggcctttcgcgcttatcaggaattgaaatcggacgatatggatcaaatgaggggaaatgatcaa	**secondary mrpD-G upshift**
U1405	ttcatcttatataacctcgtcagtatttttcaatatttttttTTAGtttttttatgaacacATTAGATATAATAAAGGGAAgattcgctatgtactatgttgat	**S633, xylR**
U1996	ttttacctgacgagtttgtaaaaaaatatttttcatattACACctgagaaattaaaggAACGAAATGTAAAAGGAAttattactgacctggataatacgctt	**yqeH, aroD, yqeI, nadD, yqeK, yqeL, yqeM**
U2030	gagattttggatatagacgaggctcttggttcacGAATTCACCAgatgtgccgtgatTACATAGTGATTATTAGAGGcgatcgaatgcaattaaatcatag	**yqzO, yqaN, S982, yqaO, S980**
U2255	cctcctctcgtcagcatgtcctatttttttatatgTATTCACGCtgcggctgaataTGAATACATTCATCTTAAAGgagggatggcatgtgtttacacaagc	**ytwI**
U2486	cggaggcaggatgacgagccacagccctctgttGGTTTGAtcgctctcctgagaGGGAAAACTGAAAGAAACGcggtcatccggcagatcgtataccatcc	**S1225; as-yukBC**
U3058	ttcagtttctcgtctatctataccggatatactcttttttTAGTGGAGaacatgtgtgtttCGCCTTATACTGAATATACAgatccttacataagagaggag	**yxkF, S1490, msmX**
U3138	agacgaggtttcttataagcctttTTCATccttttcCCTCCTTCCTTGTAAaaaaataggctatcacgcacaactaaatattataatcctctgataattct	**yxbC**

U3060	agatagacgagaaactgaaagggaaacctcattCGTTTACatattggcttcagcGGAAATAGAAGAAGACATGcaggaccaaaggagggtcatcttatgag	**aldY**
U118	tttgaaaataaaaaatttaattttcctCTTTACAAacagggggtgacctGTATATAATAACTTTTGTCAgctcgacgagaacacaacggcccgttggtcaa	**trnSL-Glu2, -Val1,-Thr1, -Tyr1, -Gln2, S67**
U301	cagcagcgatcgcggcctatgcgaatcaaaacGGATTACttttgctgacagcGGGAATTAACGGTAATATCatccgctttttgacaccgctcgtcatctca	**secondary gabD upshift**
U902	atcagactcttttgtcacctcactttctgctaaaattggaTTCCCCCTtcgcttttttgTATGGTATGATAACTTTTAGaatagaatgagaaggacgaaggtg	**yjzD, S399**
U934	acaacctctatgcttaatgttcatatttttgtcacaaAACATAacgaagtgcattcacTCATATCCTTATAAGGAAAaaggacgaggaggaccgccatgat	**yizD**
U1428	agcttacttttcataaattcaaaaatgagaagAACAGCGCCCgggctaatggtatATAATATTGTGAATTTAACAaaaatttaacaaggaggacgagagaa	**S654, yndL, S657, fosB, S658, S659**
U1534	tatagatcagaacaaaagttcgatgtaaatgttggtaataaaatataaaggtcaataatgaTATCCGTAGTATTAATAAAGgagagattcttttcgacgag	**yozM**
U1794	atttcgagcttttcacttgaactgaaaaaGGTTTGatgcgtcgggtaattGTAAATACTGTTAACGACAttgccttttttcgatgacgaggcatcaatgcc	**S869 - sporulation sRNA - as-ypdA**
U1806	taaggctctttttagttgctattcatataatagaaATTTtcaaaaaaaagttgTACGTGTATAATAAAACAAGgtaaagattgaaaggatttgagacgag	**aroC**
U1860	cagcaattcgtccttcgtctgccaattcattgattccgcccctcctaTGAATAAaaatgcttctataCTGAAAAATAAActgatttctcgtctattataca	**yqjM**
U2140	tgtaagaaaaaccgattgcatttcacaaagcttttaCGTCTAattcatgggataaggGAATACATTTTTACAAAGAcgaagccatcagcatgtctgacggtt	**yrzE**
U2221	aattgttaaaatgcgtgatatttcatcagtattCCTCGGAGCAatcacggcatcaGGCATAGACTGATACTGAGGcgtcgcatcatatgaatagacgagac	**S1083; as-ysfB**
U2256	aaacacatgccatccctcctttaagatgaatgtaTTCATAttcagccgcagcgtGAATACATATAAAAAATAGgacatgctgacgagaggaggaccgtttt	**ytvI**
U2654	tgtttctctttctatattttatcaatcacgctTGCATGCCctccctcgttattTGCGTTATAATAGTGACAGAcgaggtgaaaagtatgaaccaatcagaa	**yvaP, S1288, yvaQ**
U3003	tacggacaattcagagcatattggctcttcattgcgCCTTTtctttcaatatttgaTGCGTTAAAATGGTAACCGTgtgaaaagatgctagacgaggaaaa	**S1473, S1472, S1471, qoxA-D**
U3203	gaaggtggtcttcaaggaaaaaacgagcaggtgctcgaacagatagagcaggaaatgctagcttcggggcttgatatagaggaacagacgaggagaaggt	**internal yzzI upshift**

Subset of transcribed regions 5' of ORFs identified in Nicholas *et al.* (26) that contain the m6A motif (indicated in red). Capitalized letters and underscores indicate predicted sigma factor binding sites. Downstream transcriptional units are listed.

References

1. Bolz, N.J., Lenhart, J.S., Weindorf, S.C. and Simmons, L.A. (2012) Residues in the N-terminal domain of MutL required for mismatch repair in *Bacillus subtilis*. *Journal of Bacteriology*, **194**, 5361-5367.

2. Hall, B.M., Ma, C.X., Liang, P. and Singh, K.K. (2009) Fluctuation analysis CalculatOR: a web tool for the determination of mutation rate using Luria-Delbruck fluctuation analysis. *Bioinformatics*, **25**, 1564-1565.

3. Lenhart, J.S., Brandes, E.R., Schroeder, J.W., Sorenson, R.J., Showalter, H.D. and Simmons, L.A. (2014) RecO and RecR are necessary for RecA loading in response to DNA damage and replication fork stress. *J Bacteriol*, **196**, 2851-2860.

4. Gibson, D.G., Young, L., Chuang, R.Y., Venter, J.C., Hutchison, C.A., 3rd and Smith, H.O. (2009) Enzymatic assembly of DNA molecules up to several hundred kilobases. *Nat Methods*, **6**, 343-345.

5. Overkamp, W., Beilharz, K., Detert Oude Weme, R., Solopova, A., Karsens, H., Kovacs, A., Kok, J., Kuipers, O.P. and Veening, J.W. (2013) Benchmarking various green fluorescent protein variants in *Bacillus subtilis*, *Streptococcus pneumoniae*, and *Lactococcus lactis* for live cell imaging. *Appl Environ Microbiol*, **79**, 6481-6490.

6. Ohshima, H., Matsuoka, S., Asai, K. and Sadaie, Y. (2002) Molecular organization of intrinsic restriction and modification genes BsuM of *Bacillus subtilis* Marburg. *J Bacteriol*, **184**, 381-389.

7. Han, J.S., Kang, S., Kim, S.H., Ko, M.J. and Hwang, D.S. (2004) Binding of SeqA protein to hemi-methylated GATC sequences enhances their interaction and aggregation properties. *J Biol Chem*, **279**, 30236-30243.

8. Lu, M., Campbell, J.L., Boye, E. and Kleckner, N. (1994) SeqA: a negative modulator of replication initiation in *E. coli*. *Cell*, **77**, 413-426.

9. Nievera, C., Torgue, J.J., Grimwade, J.E. and Leonard, A.C. (2006) SeqA blocking of DnaA-oriC interactions ensures staged assembly of the *E. coli* pre-RC. *Mol Cell*, **24**, 581-592.

10. Bale, A., d'Alarcao, M. and Marinus, M.G. (1979) Characterization of DNA adenine methylation mutants of *Escherichia coli* K12. *Mutat Res*, **59**, 157-165.

11. Pukkila, P.J., Peterson, J., Herman, G., Modrich, P. and Meselson, M. (1983) Effects of high levels of DNA adenine methylation on methyl-directed mismatch repair in *Escherichia coli*. *Genetics*, **104**, 571-582.

12. Casadesus, J. and Low, D. (2006) Epigenetic gene regulation in the bacterial world. *Microbiol Mol Biol Rev*, **70**, 830-856.

13. Lee, P.S., Lin, D.C., Moriya, S. and Grossman, A.D. (2003) Effects of the chromosome partitioning protein Spo0J (ParB) on *oriC* positioning and replication initiation in *Bacillus subtilis*. *J Bacteriol*, **185**, 1326-1337.

14. Dupes, N.M., Walsh, B.W., Klocko, A.D., Lenhart, J.S., Peterson, H.L., Gessert, D.A., Pavlick, C.E. and Simmons, L.A. (2010) Mutations in the *Bacillus subtilis* beta clamp that separate its roles in DNA replication from mismatch repair. *J Bacteriol*, **192**, 3452-3463.

15. Noirot-Gros, M.F., Velten, M., Yoshimura, M., McGovern, S., Morimoto, T., Ehrlich, S.D., Ogasawara, N., Polard, P. and Noirot, P. (2006) Functional dissection of YabA, a negative regulator of DNA replication initiation in *Bacillus subtilis*. *Proc Natl Acad Sci U S A*, **103**, 2368-2373.

16. Marinus, M.G. and Morris, N.R. (1974) Biological function for 6-methyladenine residues in the DNA of Escherichia coli K12. *J Mol Biol*, **85**, 309-322.

17. Herman, G.E. and Modrich, P. (1981) *Escherichia coli* K-12 clones that overproduce dam methylase are hypermutable. *J Bacteriol*, **145**, 644-646.

18. Cooper, L.A., Simmons, L.A. and Mobley, H.L. (2012) Involvement of Mismatch Repair in the Reciprocal Control of Motility and Adherence of Uropathogenic *Escherichia coli*. *Infect Immun*, **80**, 1969-1979.

19. Lenhart, J.S., Sharma, A., Hingorani, M.M. and Simmons, L.A. (2013) DnaN clamp zones provide a platform for spatiotemporal coupling of mismatch detection to DNA replication. *Molecular microbiology*, **87**, 553-568.

20. Lenhart, J.S., Pillon, M.C., Guarne, A., Biteen, J.S. and Simmons, L.A. (2015) Mismatch repair in Gram-positive bacteria. *Res Microbiol*. 167(1):4-12.

21. Lenhart, J.S., Schroeder, J.W., Walsh, B.W. and Simmons, L.A. (2012) DNA Repair and Genome Maintenance in *Bacillus subtilis*. *Microbiology and molecular biology reviews : MMBR*, **76**, 530-564.

22. Yeeles, J.T., Gwynn, E.J., Webb, M.R. and Dillingham, M.S. (2011) The AddAB helicase-nuclease catalyses rapid and processive DNA unwinding using a single Superfamily 1A motor domain. *Nucleic Acids Res*, **39**, 2271-2285.

23. Youngman, P., Perkins, J.B. and Losick, R. (1984) Construction of a cloning site near one end of Tn917 into which foreign DNA may be inserted without affecting transposition in *Bacillus subtilis* or expression of the transposon-borne erm gene. *Plasmid*, **12**, 1-9.

24. Konkol, M.A., Blair, K.M. and Kearns, D.B. (2013) Plasmid-encoded ComI inhibits competence in the ancestral 3610 strain of *Bacillus subtilis*. *J Bacteriol*, **195**, 4085-4093.

25. Smith, B.T., Grossman, A.D. and Walker, G.C. (2001) Visualization of mismatch repair in bacterial cells. *Mol. Cell*, **8**, 1197-1206.

26. Nicolas, P., Mader, U., Dervyn, E., Rochat, T., Leduc, A., Pigeonneau, N., Bidnenko, E., Marchadier, E., Hoebeke, M., Aymerich, S. *et al.* (2012) Condition-dependent transcriptome reveals high-level regulatory architecture in *Bacillus subtilis*. *Science*, **335**, 1103-1106.